



# IGC Newsletter

## IN THIS ISSUE

### Technical Articles

- Application of Genetic Algorithms in Nuclear Fuel Management Studies
- Nanoporous Metallic Materials for Functional Applications

### Young Officer's Forum

- Single-cycle Approach for Partitioning of Minor Actinides from High-Level Liquid Waste

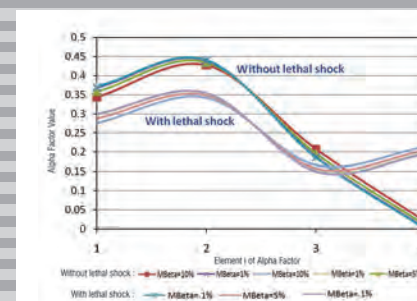
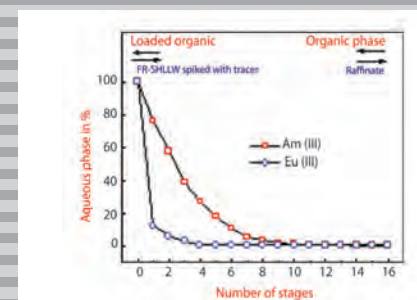
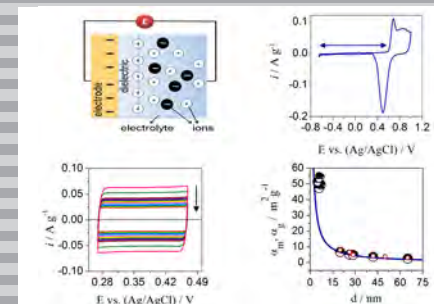
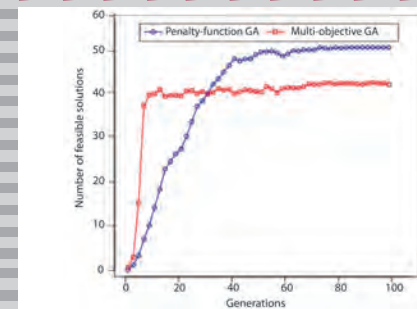
### Young Researcher's Forum

- Alpha Factor Model for Common Cause Failures Analysis of Engineered Safety Systems using Mapping Technique
- 30 kWp Grid Connected Solar Plant at ESG

### Conference and Meeting Highlights

- Inauguration of 2MIGD Reverse Osmosis Desalination Plant

### Awards & Honours



## *From the Editor*

### *Dear Reader*

It is my pleasant privilege to forward a copy of the latest issue of IGC Newsletter (Volume 107, January 2016, issue). This is the first issue coming in the New Year. I take this opportunity to wish you all a very happy New Year on my personal behalf and on behalf of the member of the editorial team.

In the first technical article, Shri M. L. Jayalal has given an account of the studies on the application of genetic algorithms in nuclear fuel management.

Dr. R. N. Viswanath has analyzed the functional applications of nanoporous metallic materials in the second technical article.

This issue's Young Officers' forum features the article by Shri Prasant Kumar Nayak, on single-cycle approach for partitioning of minor actinides from high-level liquid waste

Shri Varun Hassija has shared his experience in analyzing alpha factor model for common cause failure in engineered safety systems using mapping technique in the Young Researchers' Forum.

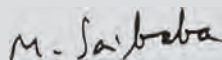
Dr. Sekhar Basu, Chairman, Atomic Energy Commission and Secretary, Department of Atomic Energy, Government of India and Director, BARC visited our Centre and during the visit he inaugurated the 2MIGD Desalination Plant.

We are happy to share with you the awards, honours and distinctions earned by our colleagues.

We look forward to your comments, continued guidance and support.

With my best wishes and personal regards,

Yours sincerely,



Chairman, Editorial Committee, IGC Newsletter

&

Associate Director, Resources Management Group

## New Year Message

### My dear colleagues,

It gives me a great pleasure in wishing you and your families a very happy, healthy and prosperous New Year 2016, full of achievements, satisfaction and glory filled with bliss. As we enter into the New Year, it is time to look back and cherish the successes of the year that passed by, having achieved considerable progress in the mission programmes of our Centre. FBTR, one of the flagships of our Centre, continues to play an important role in testing the fuel, structural materials and special neutron detectors towards development of Fast Reactor programme. During the year, 23<sup>rd</sup> irradiation campaign was completed. During this campaign, reactor was operated at its highest power level of 24.5 MWt producing 5 MWe, which was fed to TNEB grid. We started our 24<sup>th</sup> campaign a few days back. Prior to starting the campaign, four control rods along with their outer sheaths were replaced as they attained neutron fluence close to the limiting value. As part of production of Uranium-233 in FBTR, 122 Thorium sub-assemblies were loaded in the 10<sup>th</sup> and 11<sup>th</sup> rings of the core. All the short and medium term recommendations of SARCOP including post-Fukushima and seismic retrofits have been implemented. KAMINI, the only U<sup>233</sup> based operating reactor in the world, is being operated successfully for neutron radiography. It continues to provide excellent services in testing the pyro devices of all space launches, an important programme of the Department of Space. High temperature fission chambers required for neutron flux measurement of PFBR have been successfully tested at KAMINI.

We have accumulated rich experience in Post-Irradiation Examination (PIE) of irradiated FBTR components, over the years. PIE carried out on a control rod discharged from FBTR has yielded valuable information about its performance. The infrastructure of Hot cells is being enhanced for handling and examining metallic fuel and structural materials being irradiated presently in FBTR and taking up the challenging PIE of these materials.

PFBR has made significant progress during the last one year and our support continues in providing crucial inputs towards commissioning and obtaining safety clearances. I am happy that IGCAR and BHAVINI are working closely to achieve the PFBR criticality and subsequent full power generation at the earliest. Some of the major contributions to PFBR in the year passed by are: completion of trial run for transportation of six PFBR dummy fuel sub-assemblies from the Interim Fuel Storage Building to PFBR Fuel Building using a trailer, experimental studies on the performance of safety grade decay heat removal system, demonstration of in-situ regeneration of secondary cold trap, in-sodium calibration

of permanent magnet sodium flow meters, performance testing of Sonar device to measure flow induced vibration of fuel subassemblies etc.

A position paper on the need and rationale for metal fuel test reactor has been submitted to DAE for consideration of in principle approval. A conceptual core design for 100 MWt Metal Fuel Test Reactor has been evolved and that of two more oxide fuelled Commercial Breeder Reactors of 600 MWe is being evolved with improved economy and enhanced safety features meeting the GEN IV safety criteria. A 5/8<sup>th</sup> scale 90° sector model simulating the hot pool of future FBRs has been commissioned for conducting hydraulic studies in water. A new facility has also been commissioned in Engineering Hall-IV to study the flow induced vibration characteristics of a cluster of subassemblies of the core of FBR. I am happy that the expertise acquired over the period of time in the domain of Seismic Qualification experiments has been utilized in carrying out experiments for various Departmental programmes using the shake table, some of them being, spent fuel storage trays of spent fuel storage facility in Tarapur, main annunciator system prototype panel for the KAPP-3&4 and RAPP-7&8. We were able to demonstrate the life of the bellows used in the passive valves of Advanced Heavy Water Reactor (AHWR), using the in-house developed multiple bellows test facility.

The operations of CORAL have given immense experience in the design of Demonstration Fast Reactor Fuel Reprocessing Plant (DFRP) and Fast Reactor Fuel Cycle Facility (FRFCF), especially in the domain of remote handling and maintenance and in achieving product purity. All efforts are being made for early commissioning of DFRP.

Electro refining of U-Pu-Zr alloy (~20 gram scale) in molten LiCl-KCl-PuCl<sub>3</sub> electrolyte salt has been demonstrated. Also, direct reduction of 100 gram batches of uranium dioxide to uranium metal by the new molten salt (LiCl-1wt%Li<sub>2</sub>O) electrode oxidation process, has been demonstrated with conversion efficiency > 98%. Ultrasonic imaging based procedure has been developed for assessment of bond integrity of Zirconium lined ferritic steel (T91-Zr) double clad for metallic fuel applications.



Advanced alkoxyacetamide reagents have been synthesized and also the single-cycle methods for partitioning of trivalent actinides directly from fast reactor high active waste have been demonstrated. In addition, the organo-functionalized inorganic and magnetic materials have been developed and demonstrated for magnetic assisted mutual separation of lanthanides and actinides. A tin oxide based sensor capable of sensing down to 10 ppm of hydrogen in argon has been developed and has been successfully tested in FBTR. Using Electrochemical Burner and Proton Exchange Membrane based Hydrogen Sensor (PEMHS) the hydrogen released during regeneration of a cold trap was monitored, managed and accounted.

Our Centre is piloting the construction of the Fast Reactor Fuel Cycle Facility (FRFCF), an important project for the success of Fast Reactor programme in the country, and coordinating with BARC and NFC in this effort. Many milestones were reached during the year. The nuclear island is now fully geared up for the civil construction of plant buildings. Construction of Training Centre, Administration Building, Central Surveillance, Safety & Health Physics building and other service buildings are progressing very well. All the required actions have been initiated for the construction of various plants of FRFCF in a planned manner and procurement of long delivery items. I am happy that with the dedicated efforts of the limited manpower we are marching ahead and the coming year shall see fructification of these efforts and removal of the bottlenecks that are impeding faster progress.

The Centre has continued to make a mark in various domains of R&D related to fast reactors and associated fuel cycle. A number of experimental facilities have been established or commissioned during the year, the notable amongst them being the 100 tonne multi axis shake table, first of its kind in our country, RISHI (Research facility for Irradiation studies in Sodium at High temperature), an innovative out of pile test loop, with passive systems under DAE-CEA collaboration on JHR (Jules Horowitz Reactor) and a multiple fuel pin test facility, RABITS (Rupture And Ballooning In TubeS) for testing the ballooning behavior of clad tubes.

The Centre has progressed with respect to capabilities in the domain of materials development and characterization. A high chromium oxide dispersion strengthened ferritic steel clad tube has been realized and use of zirconia as an alternate dispersoid to yttria shows promise. A vanadium alloy, which could be employed for structural applications at high operating temperatures, was studied using multiple advanced electron microscopy techniques for characterization. For the first time, electron transfer process is understood in resistive gas sensing for nanostructured materials using localized scanning probe microscopy. In the area of

nano-fluids an opto-magneto-rheometer suitable for probing field-induced microstructures has been designed and developed. Non-contact electromagnetic acoustic transducers and eddy current array sensor probes have been developed for detection of sub-surface defects in austenitic stainless steels. The Electron Back Scattered Diffraction tomography, a state-of-the-art technique for study of 3-Dimensional grain morphology and orientation has been established. Micro-scanner as vision based non-contact metrology system to report shape and surface artifacts of fuel pellets and a 3-dimensional Macro Scanner for laser based profile reconstruction of spent sub-assemblies of FBRs have been developed.

We made considerable progress in the domains of Electronics and Instrumentation. Our efforts in the area of Wireless Sensor Networks have brought international acclaim. The technology developed has been transferred to ECIL for broader reach in the country. We could successfully monitor plutonium in air in collaboration with BARC. Various R&D programmes have been initiated towards I&C design of CFBR 1&2. A state-of-the-art 400 nodes, 9600 cores super computing cluster system with performance rating of 200 tera flops is being commissioned to meet the growing computational requirements for the various R&D activities of the Centre.

Successful demonstration of the Online Nuclear Emergency Response Decision Support system (ONERS) along with indigenously developed and validated source term module for the Off-Site Emergency Exercise with weather prediction system are some of the important achievements in the field of radiation safety. Environmental research in the areas such as bioremediation for uranium recovery (fresh and sea water), total trihalomethane (TTHM) estimation in fresh and sea water and surface micro layer studies are being pursued.

I am also very happy that the construction of 2 MIGD RO Desalination Plant has been completed and the plant has been commissioned. This plant would ensure supply of water to the various plants at DAE Kalpakkam Complex. It is also a very happy occasion when the plant was formally inaugurated by Dr. Sekhar Basu, Chairman, AEC and Secretary of Department of Atomic Energy. I look forward to this plant being operated to its full capacity and with high availability factor.

We have successfully completed nine years of BARC Training School programme at the Centre, which had provided valuable and capable manpower not only to our Centre but also to other Units of the Department. In the current batch, 37 Trainee Scientific Officers are undergoing training at Training School. As a constituent institution under Homi Bhabha National Institute, our Centre

at present has 167 research scholars pursuing their doctoral programmes. Further to this, 210 students from various academic institutes have carried out their project work at our Centre.

As part of commemoration of sixty years of commendable achievements of the Department, a series of programmes including lectures by eminent people, exhibitions for bringing awareness about the Departmental activities, state-level quiz competitions and lecture-cum-demonstrations on handling radioactivity were conducted during the year long celebrations.

It is my duty to acknowledge the untiring efforts being put by our technical cadres without which our projects and R&D efforts would not have been successful. The support provided by accounts and administration in smooth execution of various projects and R&D programmes is commendable.

A Vision 2030 document for IGCAR has been prepared which would

be setting the goals for the R&D to be taken up on priority in the coming years towards meeting the challenges of realizing matured fast reactor and associated closed fuel cycle technologies.

In the year ahead, I look forward to all the colleagues putting their best efforts and contribute to PFBR attaining the milestone of criticality and commercial operation, 100 MWt MFTR taking shape by getting necessary approvals, completion of preliminary design reports for CFBR 1&2, attainment of hot commissioning of DFRP, faster execution of FRFCF project etc. Efforts would be continued to tread the path of excellence in the domain of R&D in the Fast Reactor and associated fuel cycle technologies.



S. A. V. Satya Murty  
Director, IGCAR

## Indira Gandhi Centre for Atomic Research

New Year 2016



*FBTR: 30 years of successful Operation*



IGCAR

*Wish you and your family  
bliss, health and successes  
during the year 2016*



## Application of Genetic Algorithms in Nuclear Fuel Management Studies

The increasing demand for intelligent optimization and machine learning methods in the domain of nuclear reactors opened up several new avenues for the application of Computational Intelligence. The three primary branches of Computational Intelligence relevant to various nuclear applications are Artificial Neural Networks (ANN), Fuzzy Logic Systems (FLS) and Genetic Algorithms (GA). Examples of such studies are neural networks in transient identification, fuzzy logics in power controlling and Genetic Algorithms in nuclear fuel management. The studies pertaining to the application of Genetic Algorithms in nuclear fuel management have got special significance when the innovative core designs and fuel management methods of future reactors are considered.

Nuclear fuel management entails making decisions that influence how a nuclear reactor core's reactivity, neutronics flux, power, and burnup distribution vary in order to produce electrical energy in safe and cost effective ways. The cost reduction is achieved through various means: maximization of fuel cycle length, maximization of the burnup, minimization of fuel inventory, and minimization of the inventory of reactivity control material. Generally, the nuclear fuel management problem has multiple objectives and constraints. When all these objectives and constraints are considered together, some of them will conflict with the other. Any one of the final solutions represents some sort of compromise in which no further improvement in a given performance index can be obtained without a degradation in at least one of the other performance indices. Therefore, the goal of the nuclear fuel management is to identify the solution vector that suggests the best compromise among the objectives, while satisfying the given constraints.

Computational Intelligence methods like Genetic Algorithms can essentially contribute in solving the multi-objective optimization problems of nuclear fuel management. Genetic Algorithm is an optimization tool based on Darwinian Theory of biological evolution. The method was developed by John Holland in 1975 (the pioneer of evolutionary computing passed away recently, on 9<sup>th</sup> August 2015) and later popularized by one of his students, David Goldberg, who successfully applied to various practical engineering problems. During the last three decades, Genetic Algorithm found its applications increasing in various fields like data mining, image processing, pattern recognition, signal processing etc. This algorithm surpasses the more traditional methods of search and optimization in the quest for robustness. This is because Genetic Algorithm does not get trapped in local optima and also does not depend upon the existence of derivatives like calculus based methods. Further, they are much more efficient than

enumerative schemes and random search algorithms, as they do not require evaluation of a very large number of points in the search space. These advantages have made Genetic Algorithms as a suitable and efficient tool in nuclear fuel management applications.

### Optimization Procedure Based on Genetic Algorithm

The overall optimization procedure followed in the development of Genetic Algorithm for nuclear fuel management applications, considering their special features and requirements, is depicted in Figure 1. The flowchart shows the commonly followed steps of Genetic Algorithm (steps shown on the left side of the flowchart), the module representing neutronics simulation codes (the block shown on the right side of the flowchart) and the interface module in the middle. The procedure of Genetic Algorithm starts with

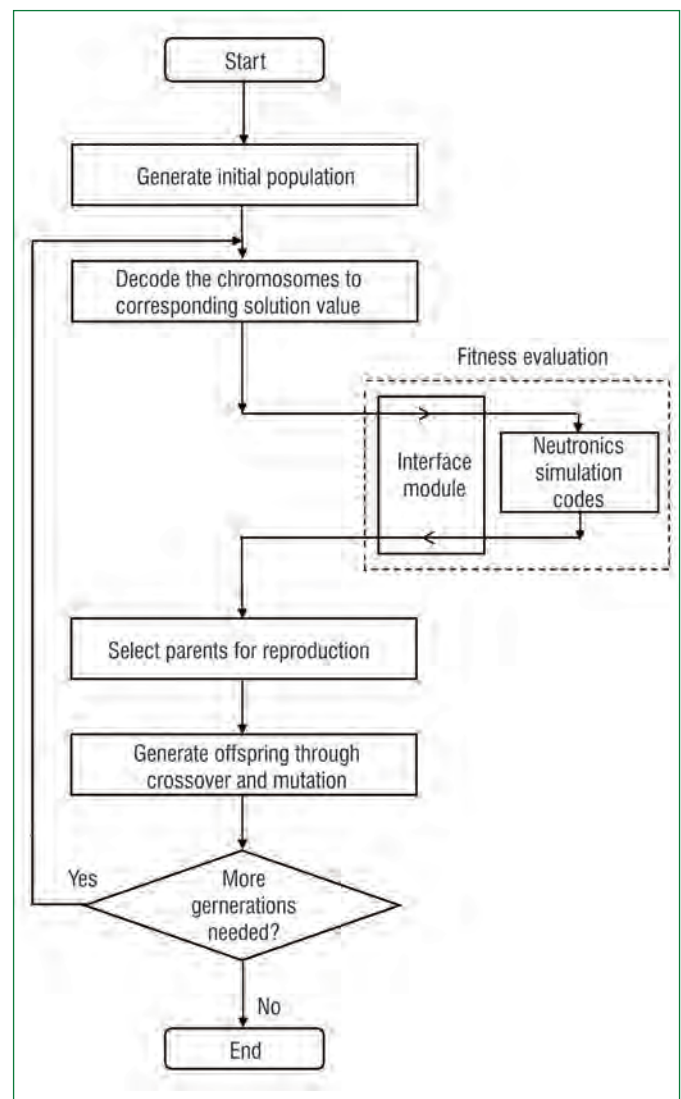


Figure1: Overall flowchart of GA based optimization procedure that is commonly followed in the nuclear fuel management applications

Table 1: Genetic parameters and methods or values used in the Genetic Algorithms based optimization procedure of burn-up optimization problem of PHWR

Parameter	Methods/Values
Encoding	Floating point
Population size	50
Crossover method	Arithmetical
Crossover probability	0.6
Mutation method	Non-uniform
Mutation probability	0.05
Maximum number of generations	100

generating a set of candidate solutions termed as “initial population” which are encoded as digital chromosomes in the algorithm.

While being executed, the fitness value of each chromosome is evaluated with the help of neutronics simulation codes. Similar to the natural selection process, chromosomes with higher fitness values have more chances of getting selected as ‘parents’ which participate in reproduction process. The ‘offspring’ solutions are produced from the parents using the genetic operations like crossover and mutation. The whole procedure of Genetic Algorithm, mentioned above, is repeated until the algorithm finds optimized results. Even though, the optimization strategies followed in different nuclear fuel management problems shares several common features, the neutronics simulation codes are specific to the type of the reactor and to the optimization problem being considered. The interface module provides a smooth communication channel between the Genetic Algorithm module and the neutronics simulation codes. In order to achieve this functionality, the interface module is equipped with efficient file handling and pattern searching mechanisms. Another important functionality of the interface module is to carry out the whole procedure in an automated way. Therefore, proper design of the interface module is an important part in the development of the overall optimization procedure.

When we come to the implementation part of Genetic Algorithm, suitable selection of the methodologies from several variants of the algorithm becomes important. By considering the special features of the nuclear fuel management problems, the two methodologies of Genetic Algorithm are selected for the present studies and are discussed in the following section.

### Genetic Algorithm Methodologies Suitable for the Nuclear Fuel Management Applications

As we have seen earlier, the optimization problems in nuclear fuel management are generally with multiple objectives and constraints. There are two flavours of Genetic Algorithm available for solving such optimization problems; they are penalty functions

based Genetic Algorithms (referred to as Penalty-function Genetic Algorithm) and Multi-objective Genetic Algorithms. In the case of Penalty-function Genetic Algorithm, the multi-objective problem of fuel management is converted into single objective by adding penalty functions and constraints. The penalty function is needed to be formulated in such a way that, it should not affect the actual objective function when constraints are not violated. On the other hand, in the case of constraint violation, the penalty function will decrement the value of objective function, in accordance with the degree of constraint violation. If the penalty coefficients and the constraints are properly selected, this approach will give feasible solutions.

In the case of fuel management applications, where the diversity in the solutions is of more importance, the multi-objective Genetic Algorithms becomes a better choice. Multi-objective Genetic Algorithm relies on the concepts of Pareto optimality and dominance. The Pareto optimal solution is the one in which an improvement in one of the objectives requires a degradation of another. The set that consists of all the Pareto-optimal solutions for a given problem forms the Pareto optimal front (or non dominated front). The method makes it possible to identify the “trade offs” between conflicting objectives in a single optimization run.

The two methodologies of Genetic Algorithm, discussed above are applied and evaluated in the selected fuel management problems of different reactor types, to arrive at the suitability of a methodology for a particular type of application. The fuel management problems considered in the present studies are optimizations of fuel bundle burn-up and core configuration.

### Optimization Study on Fuel Bundle Burn-up of PHWR

The fuel burn-up optimization of nuclear reactors helps in the maximum utilization of fissile materials without violating various safety aspects of the reactor. The optimization problem of fuel bundle burn-up, selected for the study aims at arriving at appropriate reference discharge burn-up values for the different zones of a 220 MWe PHWR core. The number of burn-up zones of the reactor core is fixed as two: an inner zone of high burn-up and an outer zone of low burn-up. The objectives selected for the optimization are: maximization of the average discharge burn-up ( $BU_{ave}$ ), maximization of the effective multiplication factor ( $K_{eff}$ ), minimization of the maximum bundle power (MBP) and minimization of the maximum channel power (MCP). The discharge burnups arrived by the Genetic Algorithm based optimization methodologies can be utilized, in fixing the most suitable reference discharge burnups for the two burn-up zones of the reactor core. The methods, parameters and values of the algorithm used in the study are given in the Table 1. The two methodologies of

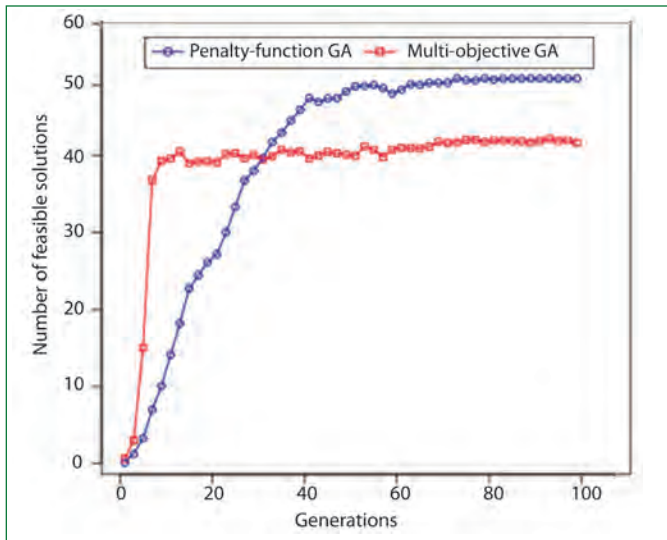


Figure 2: Average number of feasible solutions (generation wise) of the burnup optimization problem: a comparison between Penalty-function GA and Multi-objective GA

Genetic Algorithm, i.e. the Penalty-function Genetic Algorithm and the Multi-objective Genetic Algorithms, have been applied and compared. Both the Genetic Algorithm methodologies were studied in detail to ascertain their suitability for the selected problem.

The average numbers of feasible solutions produced in successive generations by the two algorithms are compared in Figure 2. This indicates a measure of “speed of convergence” of the algorithm. The average number of feasible solutions produced by considering the twenty trial runs of the penalty-function Genetic Algorithms is given in Figure 2. It can be noted from the figures that the Multi-objective Genetic Algorithms produces feasible solutions at a faster rate in earlier generations and has a better convergence speed. This implies that the total number of generations required for convergence of the optimization problem is less in the case of Multi-objective Genetic Algorithms compared with the penalty-function Genetic Algorithms.

The convergence of the given objectives during the whole evolution of the penalty-function Genetic Algorithms and Multi-objective Genetic Algorithms are plotted in Figure 3. The convergences of the four objectives for Penalty-function Genetic Algorithms are shown in Figure 3(a) to 3(d). Similarly, the convergences of the four objectives of Multi-objective Genetic Algorithms are shown in Figure 3(e) to 3(h). In the figures, the ability of the algorithms to make all the objectives converged to the feasible regions are illustrated. Further, it can be observed that the convergences of all the objectives by the penalty-function Genetic Algorithms are to narrower regions when compared with those by the multi-objective Genetic Algorithms. This behavior throws light into the ability of the multi-objective Genetic Algorithms in preserving the diversity amongst the solutions arrived.

## Optimization Study on Core Configuration of Fast Breeder Reactor

The study on optimal core configuration of Fast Breeder Reactor core explores the machine learning and computational intelligence abilities associated with Genetic Algorithms in finding the optimal number of subassemblies in the reactor core. Determining optimal core configuration of Fast Breeder Reactor is the result of detailed neutronics scoping studies, taking into consideration of several factors like, size of the core, enrichment of the fuel, linear heat rating of the fuel pins, excess reactivity of the core, control rod design and inventory requirement of the fuel. Therefore, optimization of the core configuration design is a complex task in terms of computational effort and time. The 500 MWe Prototype Fast Breeder Reactor (PFBR) core having two different fuel enrichment zones is considered in the study. The objectives selected for the optimization are: Linear Heat Rate of the inner enrichment zone (LHR1), linear heat rate of the outer enrichment zone (LHR2), excess reactivity of the core (RHO), breeding ratio achieved for the configuration (BR) and the required fuel inventory (FUI). The results obtained from the study suggest the optimal number of subassemblies in the inner and outer enrichment zones of the core to achieve the best performance of the reactor. Similar to the case of burn-up optimization of the PHWR core, the two methodologies of Genetic Algorithms, i.e. the penalty-function Genetic Algorithms and the Multi-objective Genetic Algorithms, have been applied and compared as part of the study. The method parameters and values of the algorithm used in the study are given in Table 2.

The comparison of the speed of convergence of the two Genetic Algorithms methodologies are depicted in Figure 4. The average number of feasible solutions produced by considering the ten trial runs of the penalty-function Genetic Algorithms and that of the Multi-objective Genetic Algorithms is given in Figure 4. The overall behavior of the algorithms is commensurate with the previous study of burn-up optimization of Pressurized Heavy Water Reactor (PHWR) and confirms the better speed of convergence of the Multi-objective Genetic Algorithms.

Table 2: Genetic parameters and methods or values used in the GA based optimization procedure of core configuration study of PFBR

Parameter	Methods/Values
Encoding	Floating point
Population size	40
Crossover method	Arithmetical
Crossover probability	0.6
Mutation method	Non-uniform
Mutation probability	0.025
Maximum number of generations	50



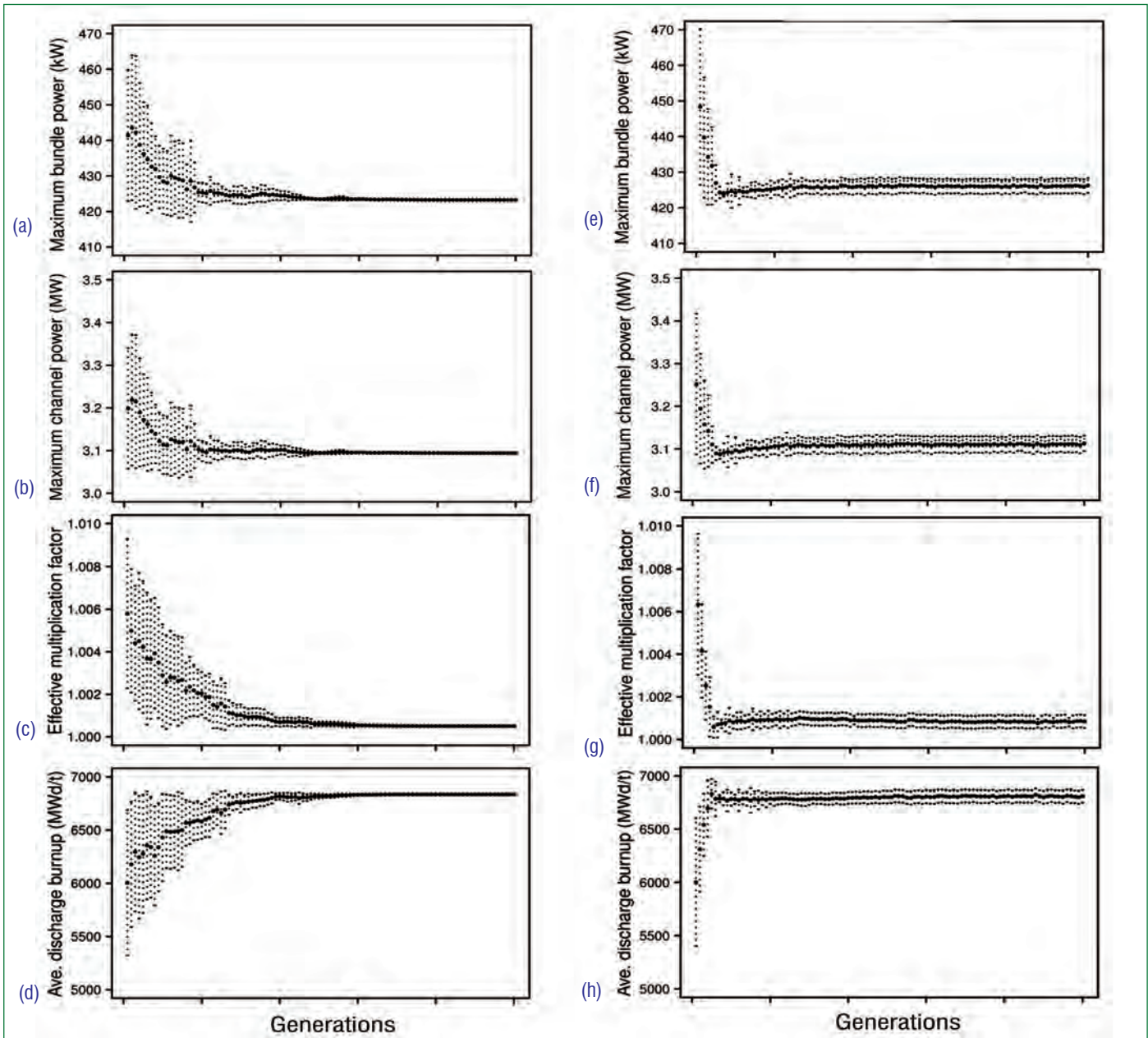


Figure 3: Convergences of the objectives during the generation wise evolution of the algorithms of the burn-up optimization problem: (a) to (d) for Penalty-function Genetic Algorithm. (e) to (h) for Multi-objective Genetic Algorithm. The solid black points denote the average value of the objective of that particular generation. The dotted lines above and below denote the standard deviation

As indicated above, the optimization problem has five objectives and the convergence of these objectives during the whole evolution of the penalty-function Genetic Algorithms and Multi-objective Genetic Algorithms are illustrated in Figure 5. The convergences of the objectives for Penalty-function Genetic Algorithms are shown in Figure 5(a) to 5(e). Similarly, the convergences of the four objectives of Multi-objective Genetic Algorithms are shown Figure 5(f) to 5(j). The important observations from the illustration are: (i) the two Genetic Algorithms methodologies are able to generate optimized solutions towards end of generations (ii) the speed of convergence of penalty-function Genetic Algorithms is comparatively slower than Multi-objective Genetic Algorithms.

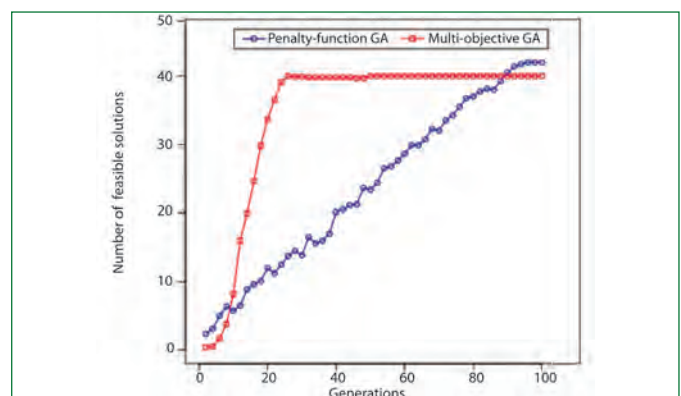


Figure 4: Average number of feasible solutions (generation wise) of the core configuration optimization problem: a comparison between Penalty-function GA and Multi-objective GA

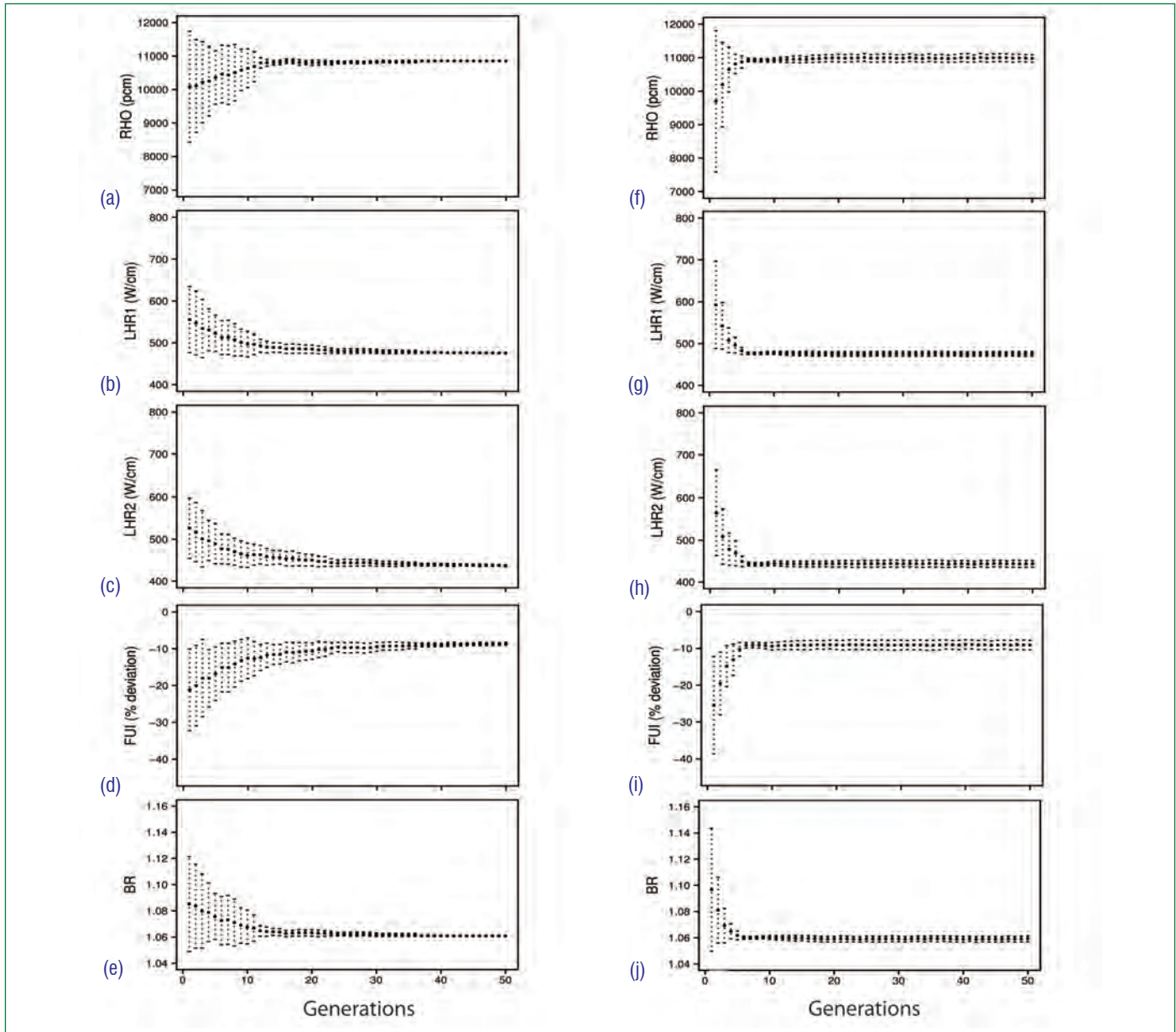


Figure 5: Convergences of the objectives during the generation wise evolution of the algorithms of the core configuration optimization problem: (a) to (e) for Penalty-function GA. (f) to (j) for Multi-objective GA. The solid black points denote the average value of the objective of that particular generation. The dotted lines above and below denote the standard deviation

### Summary and Future Directions

The application and comparison of GA based optimization methodologies with the aim of verifying their suitability, in a set of diverse nuclear fuel management studies, were carried out as part of these studies. The suitability of the selected Genetic Algorithm methodologies namely, Penalty-function GA and Multi-objective GA, are verified for different types of optimization problems of nuclear fuel management. The computational time required for the optimization of nuclear fuel management can be reduced by the application of GA. The whole procedure of complex optimization is made automated, in which the traditional way of manually changing the input parameters and analyzing the output is replaced by the generation wise evolution of the algorithm. Moreover,

the capability of intelligent optimization built into the GA allows the fuel management problem to arrive at the feasible solutions faster, without exploring the whole search space, resulting in the saving of computational time. The ability of GA in preserving diversity amongst the feasible solutions is another advantage for the fuel management. The designer of the core can go for a more informed decision-making with the help of these diverse solutions. In essence, the studies conducted have thrown open valuable insights towards the advantages and scope of applications of intelligent optimization algorithms like Genetic Algorithm in nuclear fuel management.

*Shri M. L. Jayalal and colleagues  
Electronics, Instrumentation & Radiological Safety Group*

## Nanoporous Metallic Materials for Functional Applications

Nanoporous metallic materials can be classified as sponge-like bulk solid substances analogous to well known nanoporous zeolites and activated carbon aerogels. They are considered as prototypical manifestation of bulk nanostructured materials. Nanoporous metallic materials possess specific functionalities and exhibit mechanical, chemical and physical properties sensitive to environments. These materials have remarkable tolerance to withstand exposure to extreme environments such as nuclear radiation, temperature and mechanical loads. However, ensuing long-term performance of nanoporous metallic materials in such extreme conditions still remains a challenge with regard to microstructure and chemical stabilities that dictate mechanical properties. The size of pores formed in such materials ranges from few nanometer to several tens of micrometers. The latter micro-porous materials correspond to metallic Ni/Al foams, naturally abundant biological skeletal structures and minerals in the earth. The unique combination of their high surface area-to-volume ratio, an outcome of presence of nanometer sized open porous channels, random interconnects ( $\sim 10^{15}$  interconnect per mm size cuboids) create a microstructure which provides stress shielding in nanoporous metallic materials. Thus, nanoporous metallic materials are known to exhibit superior properties as compared to their dense counterparts and micro-porous metallic foams. The present article focuses mainly on the development of nanoporous metallic materials and determination of their specific surface area. It also brings out factors influencing the stability of ligament-porous network in nanoporous metallic materials. These aspects are studied in nanoporous Au as a function of temperature and mechanical load.

Significant development has taken place in the area of nanoporous metallic materials during past two decades. There are a range of qualitative methods available for synthesising nanoporous metallic materials in bulk as well as in thin film geometries. Among them, template and electrochemical dealloying methods are widely used. Long-range ordered nanoporous metallic structure with uniform pore size and microstructure can be fabricated successfully

by the template based synthesis. However, there are limitations in using template method. This method permits neither tailoring nor modification of length scale pertaining to pores. In contrast to what is achieved by the template method, the microstructure produced by the dealloying method is random in nature and provides dynamic modulation of length scales of porous region and the thickness of the solid network. Electrochemical dealloying is primarily a corrosion involved interfacial process. It is used to produce nanoporous metallic materials from multi component alloy systems. Two most important events that occur during dealloying process are preferential dissolution of less noble element(s) present in the alloy and rearrangement of the more noble atoms in the alloy to form porous open cell architecture.

The procedure for producing bulk nanoporous metallic materials is described briefly using nanoporous Au as a model system. The alloy specimens of nominal composition  $\text{Ag}_{75}\text{Au}_{25}$  were formed from pure elemental materials, Ag and Au. Alloying was made using an arc melter under the flow of high purity Ar gas. When electrical arc is struck between tungsten and the copper hearth electrodes under Ar shroud, intense heat is released from arc plasma which brings about alloying. A photograph of an arc melter taken during the alloy formation is shown in Figure 1(a). The uniform melting of the Ag and Au mixture is seen in closed photographic view displayed at the right side of Figure 1(a). The alloy was further heated at  $800^\circ\text{C}$  for chemical micro-homogeneity and then shaped in to the required form (cylinder, disc, cuboids, sheets) using the standard metal working processes.

Dealloying experiments were carried out in 1 M  $\text{HClO}_4$  electrolyte by applying the cell potentials in the range of 0.75–0.85 V versus pseudo Ag/AgCl reference electrode. The alloy  $\text{Ag}_{75}\text{Au}_{25}$ , Ag wire and Ag/AgCl pseudo wire served as working, counter and reference electrodes respectively. Figures 1(b) and 1(c) show the photographs of a disc shaped  $\text{Ag}_{75}\text{Au}_{25}$  alloy and porous Au skeleton body obtained after complete leaching of Ag.



Figure: 1(a) Arc melting furnace set-up. (b), (c) Photographs of  $\text{Ag}_{75}\text{Au}_{25}$  alloy and nanoporous Au, respectively. (d), (e) SEM micrographs of nanoporous Au at two different magnifications

Figures 1(c)–(e) show the structure of the nanoporous Au specimen at different magnifications. The scanning electron microscope image at lower magnification (Figure 1 (d)) illustrates presence of fractured boundaries at 25–60  $\mu\text{m}$  intervals. These boundaries are assumed to be the demarcation of grain boundaries of the master alloy  $\text{Ag}_{75}\text{Au}_{25}$ . Figure 1 (e) displays the typical high resolution scanning electron microscope image of nanoporous metallic materials, revealing nanometer sized ligaments with three-dimensional open porosity. As evidenced from the microscopic results, it is inferred that even though the specimen microstructure reached lower stability limit for a stable state of condensed matter, the nanoporous Au remains monolithic up to the length scale of grains.

Open porous structure formed in nanoporous metallic materials has following advantages. Gas or fluids can flow through the pores with the support of capillary stress that acts effectively on smaller volume solids. Both catalytic activity and porous membrane fabrication require nanoporous metallic materials to have large specific surface area. Brunauer-Emmet-Teller (BET)

method is routinely used for the determination of specific surface area. Brunauer-Emmet-Teller method provides the surface area results precisely based on the analysis of adsorption isotherms. In comparison, electrochemistry based techniques are useful for measuring the specific surface area of solids in fluidic environments. Electrochemical methods have other advantages. Surface area measurements can be carried out in an electrochemical cell without exposure of the electrode materials to other environments. Electrochemical double layer (ecd) capacitance method for the specific surface area measurements is described here. An electrochemical double layer structure developed by Helmholtz is used. Its configuration is similar to an ideal two parallel plate solid state capacitor. In the electrochemical double layer, space charge region localized at the polarized electrode surface and the charged layer of ions accumulated at the electrode-electrolyte interface act as two plates and the solvent molecules that are solvated around the ions serve as dielectric. An illustration of the double layer on a noble metal surface is as shown in Figure 2 (a).

An easy way to find the double layer interface structure formed

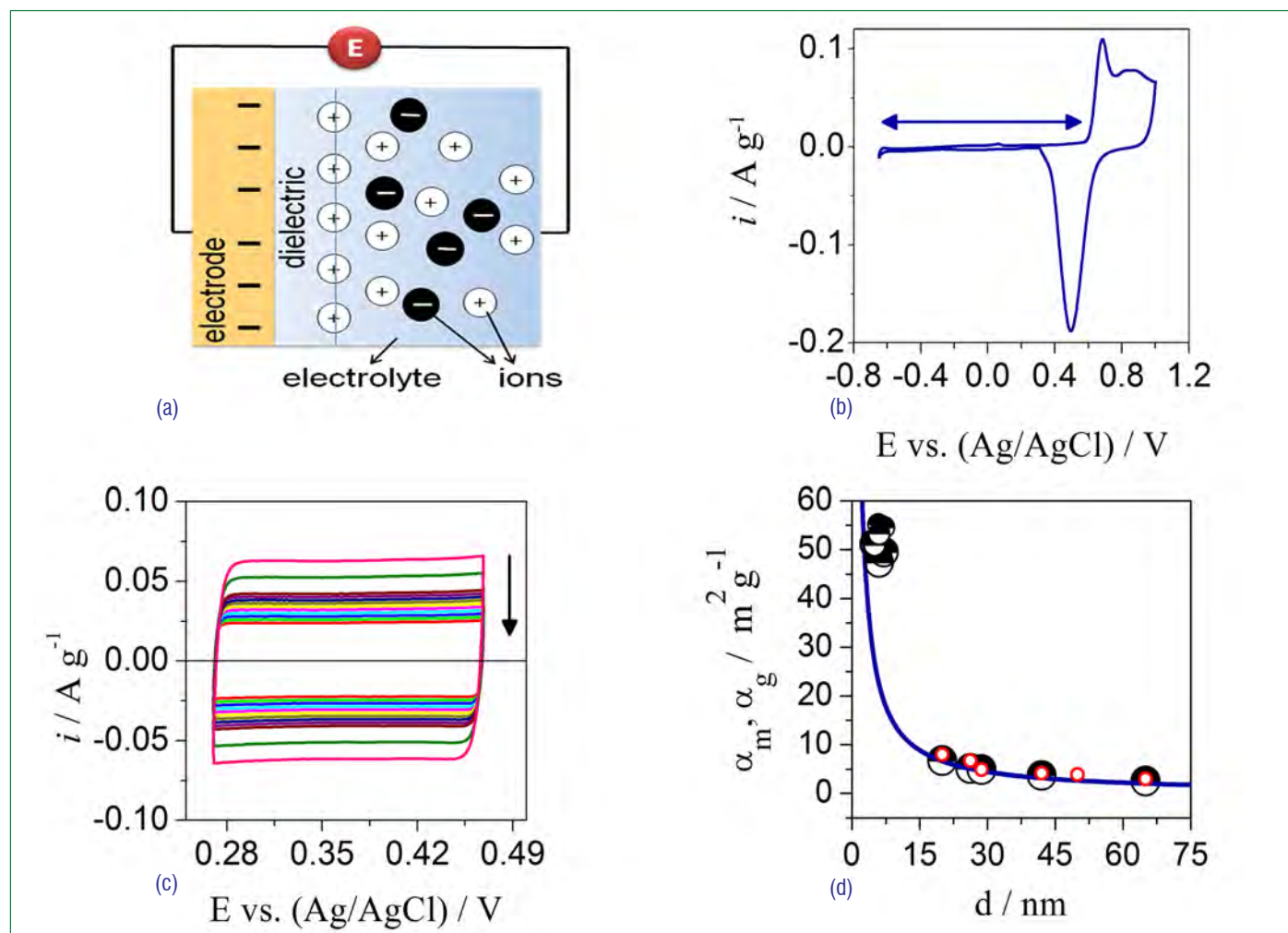


Figure 2: (a) Schematic of a double layer structure. (b), (c) Cyclic  $i$  versus  $E$  scans (d) A plot of  $\alpha_m$  (symbols  $\bullet$  and  $\circ$ ) and  $\alpha_g$  (line) versus ligament diameter for nanoporous Au

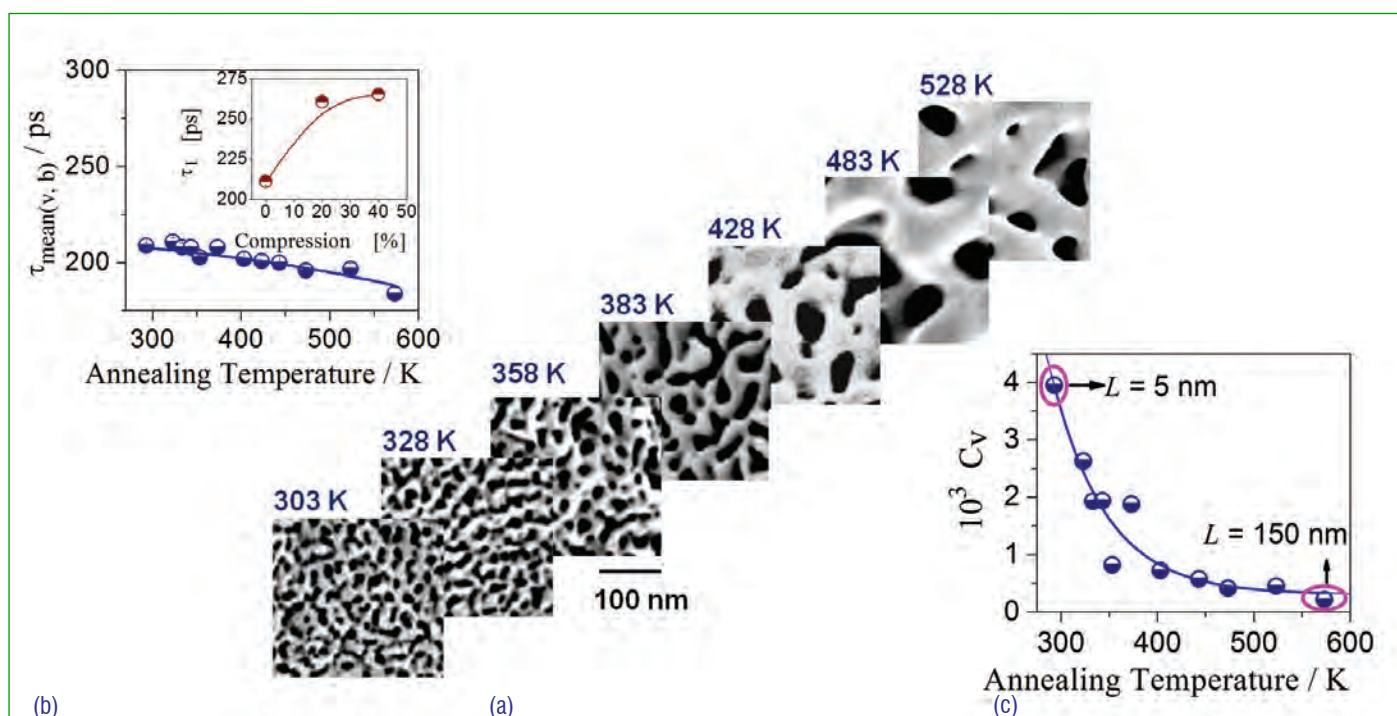


Figure 3: Evolution of microstructure and positron lifetime results of nanoporous Au up on annealing temperature. (a) Evolution of microstructure of nanoporous Au up on annealing. (b) Positron lifetime  $\tau_{\text{mean}(v,b)}$ . (c) Concentration of vacancies  $C_v$  in nanoporous Au that evolved with annealing

on an electrolyte wetted solid electrode is based on cyclic voltammetry scans. Figure 2 (b) shows a typical specific current,  $i$ , versus,  $E$ , cyclic scan for nanoporous Au in 1 M  $\text{HClO}_4$ . The scan shows a broad anion adsorption/desorption peaks at positive end of the potential range and an interval - 0.5 and 0.5 V (versus Ag/AgCl pseudo reference electrode). A small constant current in the anodic and cathodic part indicates the dominant process of double layer charging/discharging. Figure 2(c) shows the voltammetry in the double layer dominating potential region at various scan rates  $v$ . The quantity of double layer charge is estimated from  $i$  versus  $E$  scans, depicted in Figure 2 (c). This is directly proportional to the electrode surface atoms density. Therefore, one can estimate the specific surface area value for nanoporous Au from the determined double layer capacitance  $C_{dl}$  prevailing at the Au surfaces. It is noteworthy that the specific surface area value of nanoporous materials is dependent highly on its structural element size. This can be verified directly from the plot of specific-mass surface area  $\alpha_m$  value for nanoporous Au samples versus ligament diameter  $L$  (Figure 2 (d)). The continuous solid line depicted in Figure 2 (d) represents its geometrical surface area  $\alpha_g$ .

Although the nanoporous metallic materials have received considerable interest due to their importance in various applications, many challenges still remain to enhance their mechanical stability at extreme conditions. There is clear evidence from numerous research activities including our recent results that the ligament size in nanoporous Au drastically alters its strengthening behaviour. Significant research towards correlating

ligament size in nanoporous Au with pore-ligament stability for enhanced mechanical properties have been carried out. However, atomistic insight in to this aspect is still lacking. This area of research deserves further studies because the instability in the ligament size and its associated microstructure limits its use at high temperature. Microstructure analysis by scanning electron microscope coupled with positron lifetime annihilation that is sensitive to defects in solids has indeed helped us to gain further insights on this issue. Post annealing treatment has been used to alter the ligament size. Figure 3 (a) shows the high resolution scanning electron microscope images of a dealloyed nanoporous Au, and its subsequent evolution with annealing. It is seen that the ligament diameter  $L$  in nanoporous Au increases from 5 to 150 nm when the annealing temperature increases from RT to 528 K. Figure 3 (b) shows the mean positron lifetime  $\tau_{\text{mean}(v,b)}$  value that is associated with vacancy defects and the lifetime value  $\tau_b$  in bulk Au as a function of annealing temperature. While an increase in ligament coarsening with heat treatment has been demonstrated (cf. Figure 3 (a)), the mean lifetime value  $\tau_{\text{mean}(v,b)}$  decreases with annealing. It reflects that the vacancies in the Au ligaments are annealed out as the ligament diameter  $L$  increases. The concentration of vacancies,  $C_v$  per Au atom in nanoporous Au computed from the measured lifetime parameters reveal that the vacancy type defects are evolved significantly in smaller sized ligaments (Figure 3 (c)). The study explicitly suggests that vacancies present in nanoporous Au play a crucial role in controlling the stability of porous-ligament network.

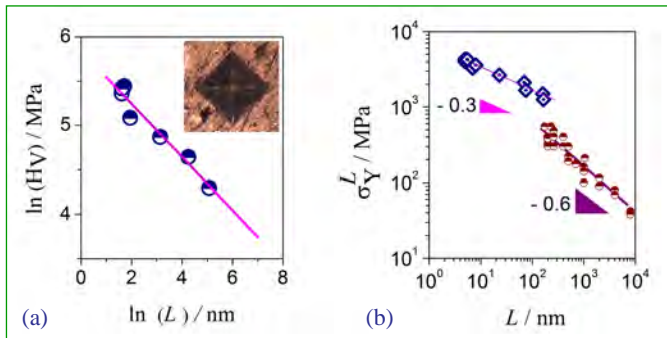


Figure 4: (a) Plot of  $\ln(H_V)$  versus  $\ln(L)$ . (b) Plot of  $\sigma_y^L$  as a function of ligament diameter  $L$

The analysis of positron lifetime spectra does not show any evidence regarding presence of dislocations in the dealloyed nanoporous Au. This finding is consistent with the growing body of evidence that lattice dislocations may not be expected in smaller volume solids. Stress levels close to the theoretical strength limit is a prerequisite for the generation of dislocations in nanomaterials. An appealing question arising at this juncture points to “while dislocations are absent in nanoporous metallic materials, whether they can be generated in the presence of mechanical load. If yes, are they sustained in the ligament network and contribute for ligament softening”. We have verified this by carrying out two independent experiments using micro hardness and positron lifetime measurements.

Different ligament sized nanoporous Au specimens were used for the hardness measurements. Hardness is a measure of resistance offered by an elastic solid medium to plastic deformation. Hence it provides information about the strengthening behaviour in solids. The hardness measurement also yields information about microstructure details from the power law exponent  $\alpha$  value in the Hall-Petch equation. Figure 4 (a) shows the Hall-Petch analysis of the variation of hardness  $H_V$  with ligament diameter  $L$ . The best fit of the  $\ln(H_V)$  versus  $\ln(L)$  curve gives a power law exponent  $\alpha$  of  $-0.3$ . It is distinctly different from the reported  $\alpha$  value of  $-0.5$  for fine grained materials. Figure 4 (b) shows the ligament yield strength  $\sigma_y^L$  in nanoporous Au obtained using the measured hardness value (cf. Figure 4 (a)), with ligament diameter  $L$ . To obtain the ligament yield strength, we used the well known density scaling equation applicable for porous materials. To see the veracity of the present observations on the ligament strength of nanoporous Au, we superposed the present results on the results obtained in earlier investigations, and these are shown in Figure 4 (b). It is seen that our results on the variation of ligament yield strength with ligament diameter (indicated by symbol  $\diamond$  in Figure 4 (b)) are in close agreement with previous reported results on nanoporous Au of smaller ligament dimensions. In a size range of 5 - 150 nm,

from the present investigations as well as the existing data from literature, a smaller exponent of  $-0.3$  is obtained.

For positron lifetime measurements, the dealloyed nanoporous Au specimens are subjected to uni-axial compression and studied. The inset in the Figure 3 (b) shows the variation of positron lifetime value in nanoporous Au along with compression. It is seen that the positron lifetime value of 209 ps in the zero compressed nanoporous Au increases to 265 ps in the 45% uni-axial compressed nanoporous Au. This large increase in lifetime value with compression can be attributed to the formation of vacancy clusters in nanoporous Au due to the movement of in-situ generated dislocations during the directional compression.

A plausible explanation for distinctive scaling exponent  $\alpha$  of value  $-0.3$  in the Hall-Petch relation, seen for nanoporous Au of smaller ligament diameter ( $< 100$  nm), can be attributed to constrained motion of dislocations along one-dimensional ligaments. The dislocations that are nucleated underneath the indentation tip/compression head flow along the ligament axis, and at the same time, there is a dislocation starvation at the ligament surfaces due to shielding stresses caused by the vacancies migrating towards the ligament surfaces which occurs as the ligament coarsens. This physical picture is substantiated by the fact that a cross over behaviour is seen when the ligament diameter becomes larger (Figure 4(b)) and the dislocation activity acquires a three dimensional character.

In summary, this article serves as a short introduction to the nanoporous metallic materials. Positron annihilation experiments demonstrated clearly that the nanoporous metallic materials can serve as sinks for absorbing vacancy defects. The combined study from scanning electron microscope coupled with positron lifetime and microhardness clearly demonstrated dimensional and microstructural constraints as well as the preponderance of free surfaces in specimen volume. These aspects collectively control the stability of ligament-porous network and the associated mechanical properties in nanoporous metallic materials. Due to these facts, these materials are considered to be one of the best candidate materials for developing prototype devices for nuclear applications. To reach the goal, new concepts in the design level have to be introduced. One of our current interests towards this direction is producing coherently coupled metallic nanoporous planar sandwich layer for efficient detection of hydrogen during steam generator leaks in fast breeder nuclear reactors.

*Dr. R. N. Viswanath & colleagues  
Materials Science Group*

## Young Officer's FORUM

### Single-cycle Approach for Partitioning of Minor Actinides from High-Level Liquid Waste

PUREX process has been adopted for the recovery of uranium and plutonium from the spent nuclear fuel. The raffinate rejected after the extraction of U(VI) and Pu(IV) is known as high-level liquid waste (HLLW). Partitioning of trivalent actinides followed by their transmutation into short-lived or stable products (P&T strategy), is vital for the safe management of high-level liquid waste. However, the separation of trivalent actinides from high-level liquid waste is a challenging task, owing to presence of chemically similar lanthanides and high concentration of nitric acid (3-4 M) prevailing in high-level liquid waste. Moreover, the presence of lanthanides also complicates the transmutation of actinides due to high neutron-absorption cross section exhibited by lanthanides. In view of this, the current approach for the partitioning of actinides is a two-cycle process. In the first-cycle, the trivalent lanthanides and actinides are co-extracted from high-level liquid waste followed by the recovery using dilute nitric acid. The second-cycle, involves the mutual separation of Ln(III) and An(III) from dilute nitric acid medium.

In contrast to this traditional approach, a single-cycle method has been developed in our laboratory, in which the actinides are separated directly from high-level liquid waste in a single processing cycle. The solvent formulation in this approach is composed of a neutral (diglycolamide) and acidic extractant (diglycolamic acid or dialkyl phosphoric acid). The trivalent actinides and lanthanides are co-extracted from high-level liquid waste by using this solvent formulation and recovery of actinides alone from the loaded solvent phase is carried out by aqueous soluble and actinide selective diethylene triamine pentaacetic acid (DTPA)-citric acid (CA) solution. Therefore, this process reduces the secondary waste generation. Based on this solvent formulations, we have



Shri Prasant Kumar Nayak, joined Irradiated Fuel Studies Section of Fuel Chemistry Division, Indira Gandhi Centre for Atomic Research, Kalpakkam after completing OCES from 4<sup>th</sup> batch of BARC training school, IGCAR campus. He has completed M. Sc. from UTKAL University, Odisha. The main areas of interest are lanthanide-actinide separation studies, minor actinide partitioning and ion exchange studies. He has over nine peer reviewed journal publications and fifteen symposium publications.

developed a couple of single-cycle approaches for partitioning of trivalent actinides that are discussed below.

#### SMART approach

Single-cycle approach for Minor Actinide partitioning using completely incinerable ReagenTs (SMART) has been explored for the separation of trivalent actinides from high-level liquid waste. This method uses the solvent formulation composed of N,N,-didodecyl-N',N'-dioctyl-3-oxapentane-1,5-diamide, (D<sup>3</sup>DODGA) neutral extractant and bis (2-ethylhexyl) diglycolamic acid (HDEHDGA) acidic extractant present in n-dodecane (n-DD). The extractants are shown in Figure 1. Since these extractants are amides and made up of CHON atoms, they are completely incinerable and the degradation products are innocuous. The distribution ratio of various metal ions present in the fast reactor simulated high-level liquid waste (FR-SHLLW) was measured in a solution of 0.1 M D<sup>3</sup>DODGA + 0.2 M HDEHDGA/n-DD.

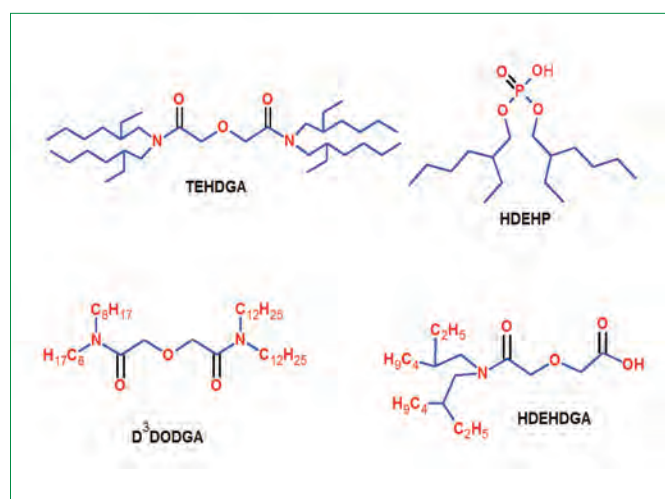


Figure 1: Structure of extractants employed in a single-cycle approach

The extraction of Am(III) was accompanied by the co-extraction of lanthanides and unwanted metal ions such as Zr(IV), Y(III), and Pd(II). Extraction of Zr(IV) was minimised by adding the complexing agent trans-1,2-diamino-cyclohexane-N,N,N',N'-tetraacetic acid (CyDTA), to FR-SHLLW. The conditions needed for efficient extraction and selective stripping were optimized.

Based on the optimized conditions, the counter-current mixer-settler run was performed in a 20-stage mixer-settler. The mixer-settler profiles show that Am(III) was quantitatively extracted in four stages. A similar extraction profile was also obtained for other lanthanides except lanthanum, which required 8-10 stages for complete extraction. Interestingly, Sr(II) exhibiting a distribution ratio of 0.51 was extracted to the extent of 90%. However, it was noted that the troublesome metal ions such as Zr(IV), Mo(VI), Fe(III), Cr(VI), Ni(II), Pd(II), Ru(III), Rh(III) were rejected to raffinate in addition to other elements.

The recovery of Am(III) from the loaded organic phase was carried out using an aqueous formulation, 0.01 M DTPA+0.5 MCA solution at pH 1.5. About 55% of Am(III) was recovered after 20 stages (product stream). It was observed that significant amount of early-lanthanides (from lanthanum to samarium) were stripped to the aqueous phase along with Am(III), where as the later-lanthanides (beyond samarium) behave similar to Eu(III). However, it should be noted that the early-lanthanides does not exhibit high neutron absorption cross-section during transmutation

of actinides. The study thus showed that recovery of Am(III) was accompanied by the stripping of "lighter lanthanides" to some extent. To minimize the stripping of lighter lanthanides, the new solvent formulation composed of a solution of N,N,N',N'-tetra-2-ethylhexyldiglycolamide (TEHDGA) and Di(2-ethylhexyl) Phosphoric Acid (HDEHP) was developed and the results of the study are discussed below. The structure of these extractants are also shown in Figure 1.

### Single-cycle approach using TEHDGA-HDEHP

Diglycolamides have been extensively employed for the extraction of Ln(III) and An(III) in the first cycle. Among the various diglycolamides, N,N,N',N'-tetra-2-ethyl hexyl diglycolamide (TEHDGA), is regarded as a promising candidate for separation of trivalent actinides from nitric acid. Similarly, the TALPEAK process was industrially demonstrated for the mutual separation of Ln(III) and An(III). This method uses di(2-ethylhexyl) phosphoric acid as extractant, which is commercially available. Since, the diglycolamide, TEHDGA in n-DD, forms third phase during the extraction of trivalent metal ions from nitric acid medium, the third phase formation behaviour of nitric acid and Nd(III) in a solution of 0.1 M TEHDGA/n-DD was studied in the presence of HDEHP. Based on the extensive studies, the concentration of HDEHP was optimized as 0.25 M in 0.1 M TEHDGA+HDEHP/n-DD. Subsequently, the solvent extraction studies of various metal ions present in the FR-SHLLW was

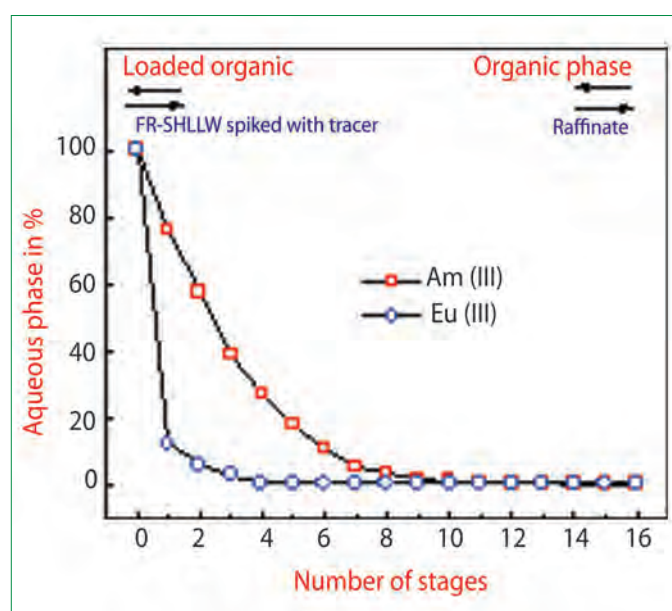


Figure 2: Profiles of Am(III) and Eu(III) extraction from FR-SHLLW using a 16-stage mixer-settler

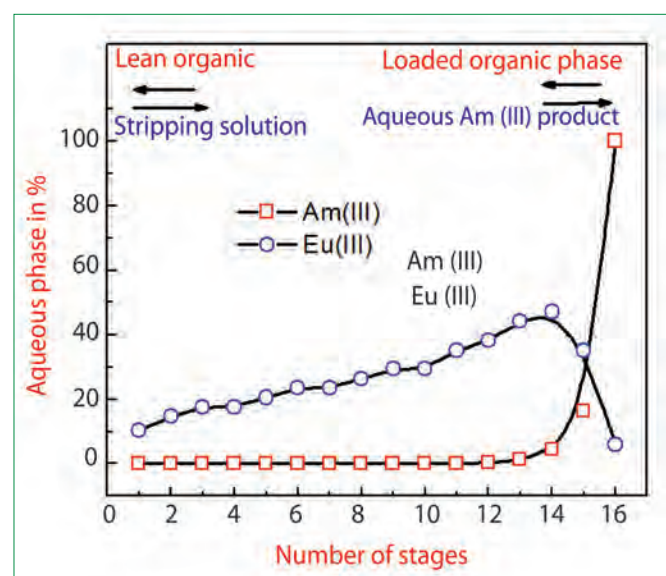


Figure 3: Profiles of Am(III) and Eu(III) stripping from the loaded organic phase using a 16-stage mixer-settler. Organic phase: Loaded organic. Aqueous phase: 0.05 M DTPA - 0.5 M CA at pH 3



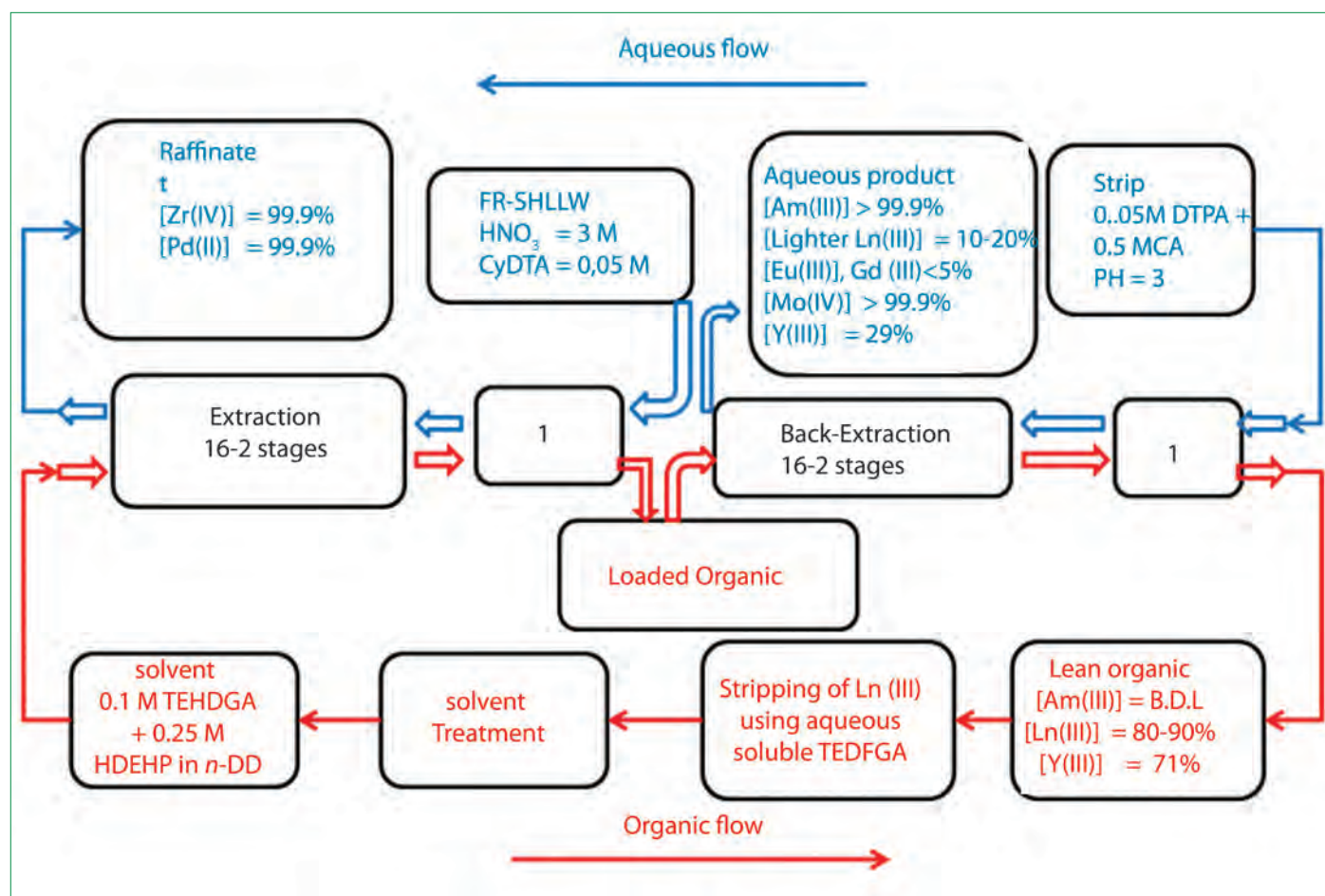


Figure 4: Proposed flow-sheet for single cycle separation of trivalent actinides from FR-HLLW using 0.1 M TEHDGA-0.25 M HDEHP/n-DD. The numbers 1 to 16 represents each mixer and settler

conducted using 0.1 M TEHDGA+0.25 M HDEHP/n-DD. Batch studies revealed that extraction of Am(III) was accompanied by the co-extraction of lanthanides and unwanted metal ions such as Zr(IV), Mo(VI), Y(III), Fe(III) and Pd(II). Similar to previous case the aqueous complexing agent CyDTA was added in FR-SHLLW to minimize the extraction of unwanted metal ions.

Based on those studies, a counter current mixer-settler run was performed to separate Am(III) from FR-SHLLW as well as from lanthanides, using a 16-stage mixer-settler. The extraction and stripping profiles are shown in Figure 2 and 3. It is observed that Eu(III) is extracted quantitatively in four stages, whereas Am(III) exhibiting lower distribution ratio than Eu(III) requires about eleven stages for complete extraction. A similar extraction profile was also observed for the extraction of other lanthanides from FR-SHLLW. It was noted that all lanthanides, Mo(VI) and Y(III) are extracted quantitatively from FR-SHLLW in 0.1 M TEHDGA + 0.25 M HDEHP/n-DD, and Fe(III) was extracted to the extent of 80%. Other metal ions were rejected to raffinate.

The recovery of Am(III) from the loaded organic phase was carried out by using 0.05 M DTPA -0.5 M CA acid at pH 3 using same mixer settler in a separate run. The stripping profile is shown in Figure 3. The stripping of Am(III) was quantitative. However, the americium product contained about 10% of lighter lanthanides i.e. lanthanum to neodymium, perhaps due to the presence of these lanthanides in high concentration in FR-SHLLW. The contamination of heavier lanthanides was less than 5%. In addition to this Y(III) and Mo(VI) were stripped to the extent of 29 and 100% respectively. However, these elements do not interfere in the transmutation of Am(III) as neutron absorption cross section for these elements is less. Our results, thus confirmed the possibility of separating Am(III) directly from FR-SHLLW in a single-processing cycle, for facilitating the transmutation of americium. The proposed flow-sheet for the selective separation of trivalent actinides from HLLW is presented in Figure 4.

Shri Prasant Kumar Nayak  
Chemistry Group

## Young Researcher's FORUM

### Alpha Factor Model for Common Cause Failure Analysis of Engineered Safety Systems using Mapping Technique

Probabilistic Safety Assessment (PSA) is a systematic and comprehensive methodology to evaluate risks associated with every life-cycle aspect of a complex engineered technological entity such as a facility, a spacecraft, or a nuclear power plant. The probabilistic safety assessment has emerged as an increasingly popular analytical tool among various industries in the last couple of decades as it provides quantitative results and qualitative insights that help to make decisions regarding design and operational issues from safety view point. In nuclear industry, it is prominently used as a tool in design optimization studies and as a regulatory tool to assess, evaluate and enhance safety of the plant.

In nuclear safety systems, redundancy is the fundamental technique adopted for fault tolerance. However, in redundant systems, Common Cause Failures (CCF) are considered to be the major contributor to risk and therefore quantifying common cause failure is essential to demonstrate the reliability of a system. In this context, various methods such as Beta factor, Multiple Greek Letter, Binomial Failure Rate, Alpha Factor are developed. The Beta factor model is a single parameter model and it assumes that whenever a common cause failure event occurs, all components within the common cause failure group fail. This model assumes that a constant fraction beta of the component failure can be associated with the common cause events shared by other components in that group. In Multiple Greek Letter model other parameters in addition to the beta factor are introduced to account more explicitly for higher order redundancies and to allow for different probabilities of failure of subgroups of the common cause component group. Binomial Failure Rate model estimates multiple



Shri Varun Hassija got his M.Tech in Nuclear Engineering from School of Nuclear Energy, Pandit Deendayal Petroleum University in 2011. He joined IGCAR as DGFS-PhD Fellow in September, 2011 and pursued his doctoral work at Reactor Design Group and AERB- Safety Research Institute under the guidance of Dr. K. Velusamy and Dr. C. Senthil Kumar. He has submitted his doctoral thesis titled as "Development and Application of Probabilistic Safety Assessment Methodologies for estimating Risk from Nuclear Power Plants" to Homi Bhabha National Institute in November, 2015. His areas of research are Probabilistic Safety Assessment and Reliability Analysis.

failure probabilities by postulating a shock that impacts the system at certain frequency to cause multiple failures. The Alpha factor model defines common cause failure probabilities from a set of failure frequency ratios and the total component failure probability  $Q_T$ . Amongst all the common cause failure models, Alpha factor is considered to be more realistic as it can model the real scenario to a greater extent. Alpha factor method does not assume that in each common cause failure event all components share the common cause but assigns probabilities to the different degrees of the cause and is based on clearly formulated probabilistic assumptions. Thus, this approach poses a more complex structure to determine the Alpha factors when the level of redundancy increases. One main advantage of this method is the ability to analyze various common cause failure events of different intensity as applicable to plant/system specific requirements. Common cause failure quantification based on common cause failure impact rate, number of components of the common cause component group affected has shown realistic behaviour of the model and is found suitable for high redundant systems. Mapping up technique enables the estimation of common cause failure basic event probability in a highly redundant system based on the plant specific data available for lower redundant system. In this work, an attempt is made to exhibit the technique of mapping up of event impact vectors to determine Alpha factor for high redundant systems. An impact vector is a numerical representation of a common cause failure event. Alpha factors are then used to estimate the common cause failure contribution to the system. A comparison of Alpha factor method and Beta factor method is also presented taking insights from the case study of the safety system of an Indian Nuclear Power Plant.

### Common Cause Failure Event

A common cause failure event is a result of simultaneous failure of two or more individual components failure due to a single shared cause, thus defeating redundancy or diversity which is intentionally employed to improve reliability of the system. Such events can significantly affect the availability of safety systems.

### Estimation of Common Cause Failure Probability

In the present study, the parametric Alpha Factor model is chosen because this model can handle common cause component group sizes of different levels and is more accurate compared to other parametric models.

The Alpha factor model estimates the common cause failure frequencies from a set of ratios of failure and the total component failure rate. The parameters of the model are

$Q_T$  = total failure probability of each component (includes independent and common-cause events)

$\alpha_k^{(m)}$  = fraction of the total probability of failure events that occur in the system involving the failure of k components in a system of m components due to a common-cause.

The common cause failure basic event equation for any k out of m components failing in case of staggered testing is given by equation 1:

$$Q_{CCF} = Q_T \sum_{i=k}^m \binom{m}{i-1} \alpha_i^{(m)} = Q_T \sum_{i=k}^m \binom{m}{i} \alpha_i^{(m)} \quad (1)$$

where:

$\alpha_i^{(m)}$  = ratio of i and only i common cause failures to total failures in a system of m components

m = number of total components in the component group

k = failure criteria for a number of component failures in the component group

$Q_T$  = random failure probability (total)

$Q_{CCF}$  = failure probability of k and greater than k components due to common cause failures.

### Estimation of Alpha Factor

A technique has been proposed by NUREG/CR-5485 for

common cause failure analysis using 'event impact vector'. An impact vector is a numerical representation of a common cause failure event and is classified according to the level of impact of common cause events. In this technique, the impact vectors are modified to reflect the likelihood of the occurrence of the event in the specific system of interest. This method is also known as mapping. The mapped impact vectors are finally used to arrive at Alpha factors. For a common cause component group of size m, an impact vector will have m elements and the  $k_{th}$  element is denoted by  $P_k$ . Here  $P_k$  denotes the probability of k component failing due to a common cause. For e.g., the impact vector a common cause component group of size 4, is

$$[P_1^{(4)} P_2^{(4)} P_3^{(4)} P_4^{(4)}]$$

### Estimation of Alpha Factors from Impact Vectors

The number of events in each impact category ( $n_k$ ) is calculated by adding the corresponding elements of the impact vectors as represented in equation 2.

$$n_k = \sum_{j=1}^n P_k^{(j)} \quad (2)$$

where:  $P_k(j)$  = the  $k_{th}$  element of the impact vector for event j, and n is the number of common cause failure events.

Finally, the Alpha factors are estimated using the equation 3:

$$\alpha_k^{(m)} = \frac{n_k}{\sum_{k=1}^m n_k} \quad (3)$$

The application of Alpha factor technique in common cause failure analysis is further demonstrated with the help of an application to Indian nuclear power plant. A MATLAB code is developed to estimate the Alpha factors and then compute common cause failure contribution to total failure probability.

### Applications to Nuclear Power Plant: Safety Grade Decay Heat Removal System of Prototype Fast Breeder Reactor

The 500 MW Indian pool type Prototype Fast Breeder Reactor (PFBR), is provided with two independent and diverse Decay Heat Removal (DHR) systems viz., Operating Grade Decay Heat Removal System (OGDHR) and Safety Grade Decay Heat Removal System (SGDHR). Operating Grade Decay Heat Removal System utilizes the secondary sodium loops and Steam-Water System with special decay heat removal condensers for DHR function. A passive Safety Grade Decay Heat Removal system using four completely independent thermo-siphon loops in natural convection mode is provided to ensure adequate core cooling for all Design Basis Events.

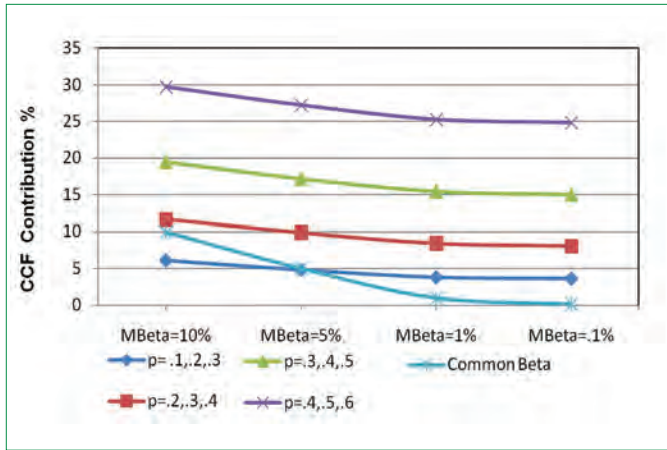


Figure 1: Common Cause Failures contribution in 2 out of 4 system without lethal shock

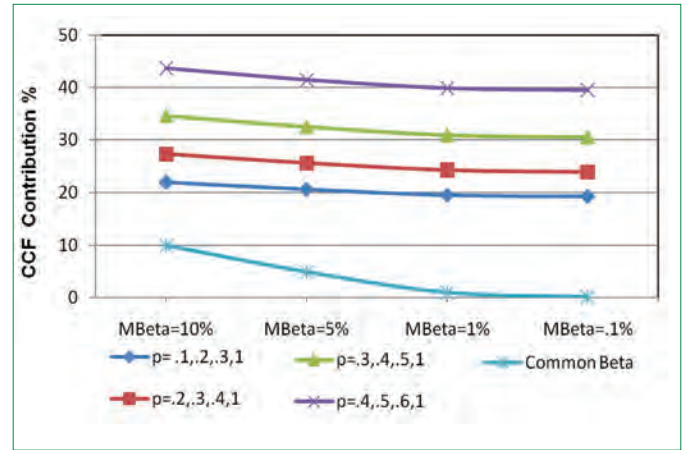


Figure 2: Common Cause Failures contribution in 2 out of 4 system with lethal shock

Since Safety Grade Decay Heat Removal is a passive system, the functional failure probability depends on the time up to which two loops are available. The event simulated in this study demand operation of two Safety Grade Decay Heat Removal loops for initial 24 hours and subsequent availability of one loop till 720 hours after the shutdown for successful decay heat removal of the reactor.

In the present study the effect of three non-lethal common cause failure events affecting the Safety Grade Decay Heat Removal system have been studied for various values of  $\rho$ . The objective of the case study is to first estimate the Alpha factors

and then arrive at the contribution of the common cause failure events to total failure probability of the system. The case when an additional common cause failure event is a lethal shock has also been analysed to study the effect of lethal shock. Finally, a broad comparison between the Alpha factor method and Beta factor method for their assessment of common cause failure contribution to total failure probability of the system due to various common cause failure events is made. Since the mapping up is performed from two component data, a term 'mapping up beta' (denoted as MBeta) is used which is expressed as the fraction of total failure

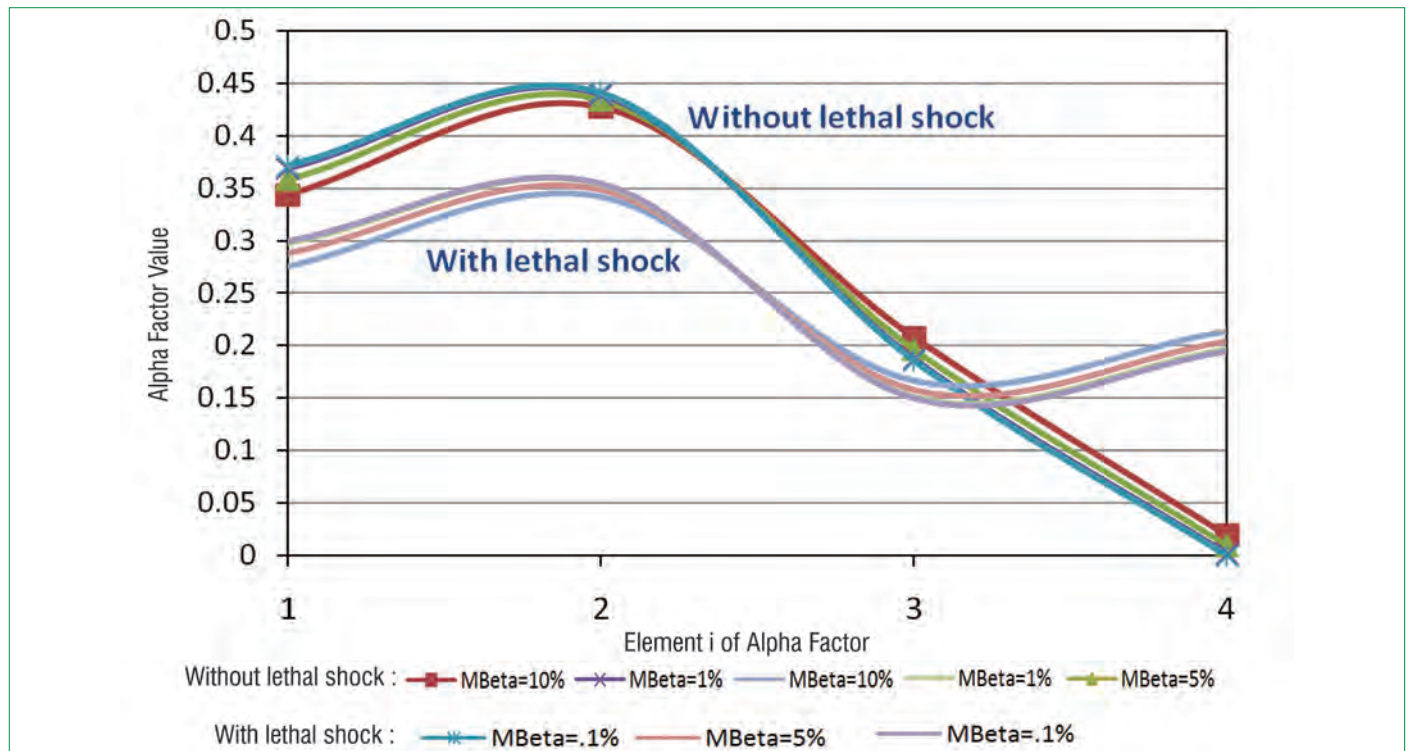


Figure 3: Comparison of a Alpha Factors for lethal and non-lethal shock

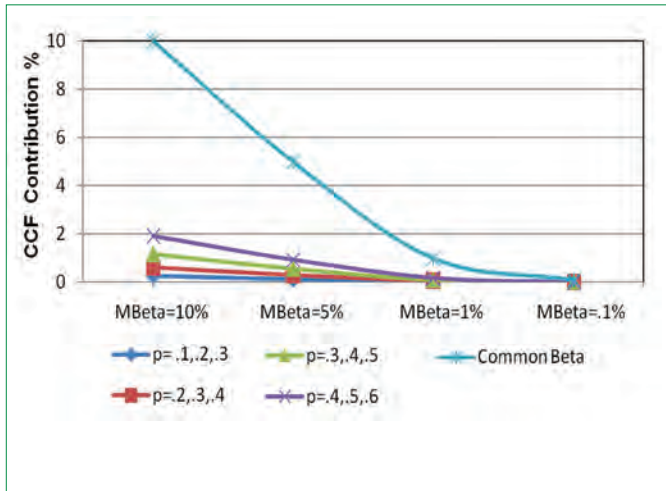


Figure 4: Common Cause Failures contribution in 1 out of 4 system without lethal shock

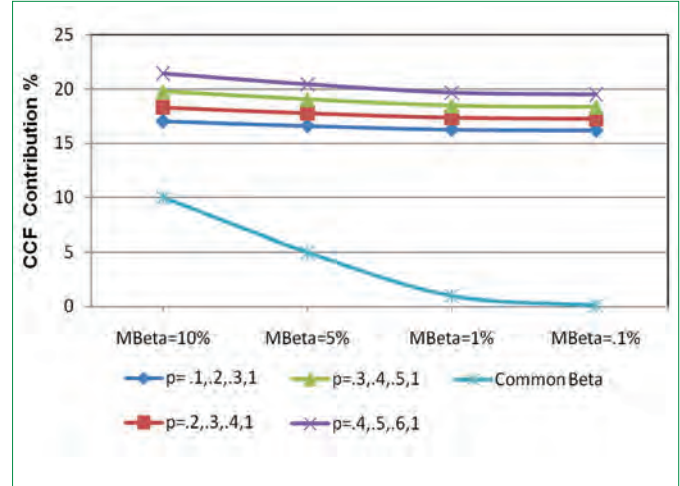


Figure 5: Common Cause Failures contribution in 1 out of 4 system with lethal shock

probability of the two component system attributable to dependent failure. It is expressed in equation 4.

$$\text{Mapping up Beta} = Q_m / Q_t \quad (4)$$

where,

$Q_m$  = Dependent failure probability and

$Q_t$  = Total failure probability for each component

Another term 'Common Beta' is also used to denote common cause failure for the complete system. Beta expressed in percentage is the common cause failure contribution to total failure probability in these cases.

The case is studied under two parts. Part one for the first 24 hours of mission time when the success criterion is two out of four and part two for rest of the mission time when success criterion is one out of four.

**When two out of four loops are required**

After the shutdown of the reactor for first 24 hours two loops of Safety Grade Decay Heat Removal are required. The contribution of common cause failure events to total failure probability for various set of values of  $\rho$  is presented in Figure 1. The results of the case with extra common cause failure event as lethal shock is presented in Figure 2.

Alpha factors as obtained for  $\rho$  value of 0.4, 0.5, 0.6 with and without consideration of lethal shock for different MBeta values are presented in Figure 3.

**When one loop is required out of four**

This case is applicable after the first 24 hours of shutdown of the

reactor till the end of mission time (720 hours). The contribution of common cause failure events to total failure probability for various set of values of  $\rho$  is shown in Figure 4. The case with extra common cause failure event as lethal shock is given in Figure 5.

The study carried out clearly indicates that Alpha factor model can be used to realistically estimate the contribution of common cause failure events to the total system failure probability. The model assesses the contribution of each of the common cause failure event based upon subjective assessment of a constant  $\rho$  which is conditional probability of each component failure given a shock. The values of a Alpha factors are found to be less sensitive to change in the value of mapping up beta and this sensitivity further reduces with more number of components added to the system. Contribution of common cause failure events to total failure probability is also found to be less sensitive to the value of mapping up beta but it is highly sensitive to the change in success criterion for the system.

The use of Alpha factors is found to be highly suitable, especially for the cases exhibiting large redundant configuration and with a requirement to meet a stringent success criteria. It is also demonstrated that the use of Beta factor model in these cases yields highly repressed estimates of common cause failure contribution especially when the lethal behaviour of common shocks is high, thereby underestimating the risks imposed by common cause events.

*Shri Varun Hassija  
Reactor Design Group*

## 30 kWp Grid Connected Solar Plant

Grid connected solar system is an emerging technology to harvest solar incident radiation for production of electricity which can be fed to the grid directly. As part of the energy conservation activities as well as considering the importance the Government of India has given to harness Solar Energy, our Centre has initiated projects in this line. To start with, a pilot plant of 30 kWp grid connected solar plant is installed and commissioned on 14<sup>th</sup> August 2015 on the roof top of ESG annex building.

### Features

On an average, this system, produces 120 to 150 units of electricity per day. On days with good solar insolation the production clocked 175 units. This is the largest solar system installed at Kalpakkam so far. All the operations are automatic and no manual intervention is envisaged for normal operation. It is not provided with any battery backup as the electricity generated is transferred to the grid on real time basis and no storage is necessary. This arrangement will ensure better efficiency at a lesser capital and maintenance cost.

### Components of the system

#### a. Solar Photovoltaic Modules (SPV Modules)

It comprises of 120 numbers of Crystalline Silicon type solar modules. Each module has an output 250 Wp. Twenty numbers of Solar Photovoltaic Modules are connected in series to form one array. Totally there are six such arrays.

#### b. Array Structure

Array structure is made of hot dipped galvanised iron and it holds the Solar Photovoltaic Modules. This structure is designed to withstand a wind speed of 200 Km/hour.

#### c. DC Distribution Box

DC distribution box receives DC output from the array field. There is a provision for voltage and current measurement from different arrays so as to check any failure in the array field.

#### d. Grid Interactive Inverter

It converts DC power produced by Solar Photovoltaic modules, into AC power and adjusts the voltage and frequency levels to suit the local grid conditions. The inverter works in fully automatic mode and is provided with an automatic synchronisation unit. In a short time after the sunrise the inverter gets activated and synchronises the solar system with the grid. With this the export of the power produced to grid starts. In the evening towards sunset the inverter disconnects from the grid and switches into sleep mode.

This system also has a built in Maximum Power Point Tracker (MPPT). Maximum Power Point Tracker ensures that the Solar Photovoltaic modules operate on the maximum efficiency point of the V - I characteristics of the module. Maximum Power Point Tracker also adjusts the voltage of the module in such a way that the power produced will be maximum. This is carried out on real time basis. There is also a facility to store the records and display the same.

#### e. AC Distribution Box

AC Distribution box receives AC power from Grid Interactive Inverter and feeds power to the grid. It also has the facility to measure the voltage, current, power, energy, power factor and frequency. After observing the performance of the already commissioned pilot project, three more similar systems with approximately 120 kWp is proposed to be implemented.

*Shri A. Jyothish Kumar*  
*Engineering Services Group*



Figure 1: Solar Photovoltaic Panels at the roof top of ESG Annex Building

## Conference and Meeting Highlights

### Inauguration of 2MIGD Reverse Osmosis Desalination Plant

18 December, 2015



Dr. Sekhar Basu, Chairman, AEC, Secretary, DAE & Director BARC, along with Dr. S. A. V. Satya Murty, Director, IGCA and senior colleagues of the Centre during the inauguration of the 2 MIGD Reverse Osmosis Desalination Plant

A two-stage 2 MIGD Sea Water Reverse Osmosis desalination plant has been commissioned recently with a flexible capacity in operation and maintenance to suit the varying demand of water in different seasons. This plant was inaugurated by Dr. Sekhar Basu, Chairman, Atomic Energy Commission, Secretary, Department of Atomic Energy, Government of India and Director, BARC on 18 December, 2015 in the presence of Dr. S. A. V. Satya Murty, Director, IGCAR, Dr. P. Chellapandi, CMD, BHAVINI, Shri T. J. Kotteeswaran, the then Station Director, MAPS, Shri Amitava Roy, Facility Director, BARC-F, Dr. P. R. Vasudeva Rao, RRF and former Director, IGCAR and

senior colleagues from IGCAR and from other Units of the Department.

The inauguration function started with a welcome address by Dr. S. A. V. Satya Murty, Director, IGCAR, followed by Shri A. Jyothish Kumar, Director, ESG, briefing the audience about the successful commissioning of the 2 MIGD sea water reverse osmosis desalination plant at IGCAR, Kalpakkam. Shri G. Kempulraj, Head, CWD, ESG delivered the vote of thanks.

*Reported by M. Sai Baba,  
Associate Director, RMG*



2MIGD Reverse Osmosis Desalination Plant



Piping and Filtration Chambers

## DAE Awards

Department of Atomic Energy has instituted annual awards for excellence in Science, Engineering and Technology in order to identify best performers in the area of Research, Technology Development and Engineering in the constituent units (other than Public Sector Undertakings and Aided Institutions). The Young Applied Scientist, Young Engineer, Young Technologist, Homi Bhabha Science and Technology Award and Scientific and Technical Excellence Award fall under this category. Group Achievement awards for recognition of major achievements by groups have also been instituted. Life-time Achievement Award is awarded to one who has made significant impact on the DAE's programmes. They are the icons for young scientists and engineers to emulate. The awards consist of a memento, citation and cash prize.

The recipients of the Awards from IGCAR for the year 2014 are:

<b>Scientific and Technical Excellence Award</b>	: Shri A. Palanivel, RDG Shri A. John Arul, RDG
<b>Young Applied Scientist / Technologist Award</b>	: Shri Barid Baran Lahiri, MMG Shri Satyabrata Mishra, RpG
<b>Young Scientist Award</b>	: Dr. Arun Kumar Rai, MMG
<b>Young Engineer Award</b>	: Shri A. Viswanath, MMG Shri Sanjeev Kumar, RDG Shri T. Raj Kumar, RDG Shri Juby Abraham, RDG
<b>Meritorious Technical Support Award</b>	: Shri G. Ramadoss, ESG Shri P. Bakthavachalam, FRTG Shri K. Arumugam, ROMG Shri R. Rajaram, CG
<b>Meritorious Service Award</b>	: Ms. Shanthi Rajendran, FRTG Ms. Sasikala Manohar, MSG

### Group Achievement Awards:

Development of Indian Reduced Activation Ferritic Martensitic (INFRAFM) Steel for India's Test Blanket Module (TBM) in ITER

Dr. T. Jayakumar, Group Leader

Dr. Arun Kumar Bhaduri, Dr. K. Laha, Dr. Saroja Saibaba, Shri Raju Subramanian, Dr. R. Sandhya, Dr. V. S. Srinivasan, Dr. Aniruddha Moitra, Dr. A. Nagesha, Dr. Vani Shankar, Dr. R. Mythili, Shri Sunil Goyal, Shri M. Nandagopal, Shri G. V. Prasad Reddy, Shri V. David Vijayanand, Ms. J. Vanaja, Shri Arun Kumar Rai, Shri Aritra Sarkar, Shri K. Mariappan, Shri N. S. Thampi, Shri R. Balakrishnan, Ms. S. Panneer Selvi, Shri M. Govindasamy from **MMG**



### Design and Development of Wireless Sensor Networks for Nuclear Facilities

Dr. S .A. V. Satya Murty, Group Leader

Ms. Jemimah Ebenezer, Shri Sukant Kothari, Ms. D. Baghyalakshmi, Ms. G. Sandhya Rani, Ms. Vinita Daiya, Shri T. S. Shri Krishnan, Ms. Deepika Vinod, Ms. R. Vijayalaxmi, Dr. R. Baskaran, Shri V. Gopalakrishnan, Dr. M. T. Jose, Shri R. Nandakumar, Shri N. Radhakrishnan, Shri V. Balu, Shri Ibrahim Khan, Shri P. Solai Raj, Shri A. Boopalan, Shri N. Sathish Kumar, Shri K. Rajesh from EIRSG, Shri S.Vannia Perumal, Shri P. Venkatesh, Dr. B. Prabhakara Reddy from CG, Shri T. Chandran, Shri M. Shanmugavel, Shri B. Babu from FRTG, Shri Kalyan Rao Kuchipudi, Shri D. Loganathan, Shri R. Shunmugavel, Shri P. Immanuel Stephen from ROMG

### Experimental Verification and Qualification of Equipment towards Demonstrating Safety of Sodium Systems of PFBR

Dr. D. Ponraju, Group Leader

Shri P. Selvaraj, Shri B. K. Nashine, Shri E. Hemanth Rao, Shri S. S. Ramesh, Shri Sanjay Kumar Das, Ms. G. Punitha, Shri Arjun Pradeep, Ms. G. Lydia, Ms. B. Malarvizhi, Shri M. Kumaresan, Shri S. S. Murthy, Shri Anil Kumar Sharma, Shri S. Athmalingam, Shri V. Balasubramaniam, Shri P. Mangarjuna Rao, Shri S. Srinivasan, Shri K. E. Jebakumar, Shri Ch. S. S. S. Avinash, Shri Avinash Kumar Acharya, Ms. V. Snehalatha, Shri G. Venkat Reddy, Shri S. Muthu Saravanan, Shri J. Anandan, Shri T. Lokesh, Shri V. Sebastia John, Shri S. Satheesh Kumar, Ms. Sujithra, Shri R. Suresh Kumar, Shri M. Aravind, Shri R. Manu from RDG, Shri V. Venkatachalapathy, Shri N. Suresh, Shri M. K. Satheesh Kumar, Shri D. Balamurugan, Ms. R. Thilakavathi, Shri D. Hari, Shri G. Ramanathan, Shri P. Senthil Arumugam from ESG, Shri T.V. Maran, Shri K. Mohan Raj, Shri S. Chandramouli, Shri G. Kempul Raj, Shri R. Iyappan, Shri R. Parandaman, Shri S. Kannan, Shri P. Lakshmayya, Shri P. Pothi from FRTG

### Design, Development and Experimental Testing of Sodium Submersible Annular Linear Induction Pump (SALIP) for FBR

Shri B. K. Nashine, Group Leader

Shri B. Babu, Shri K. V. Sreedharan, Shri B. K. Sreedhar, Shri S. Chandramouli, Shri G. Vijayakumar, Ms. J. I. Sylvia, Shri V. Ramakrishnan, Shri S. K. Dash, Shri Prashant Sharma, Shri Vijay Sharma, Shri R. Rajendra Prasad, Shri Gautam Anand, Shri S. Kannan, Shri R. Iyyappan, Shri P. Lakshmayya, Shri P. Pothi, Shri P. Vijaya Mohan Rao, Shri G. Anandan, Shri P. Bakthavatchalam, Shri V. Krishnamoorthy, Shri Pitambar Padhan, Shri A. Ashok Kumar, Shri S. Krishnakumar, Shri Parmanand Kumar, Shri N. Venkatesan, Shri A. Thirunavukkarasu, Shri P. C. V. Murugan, Shri N. Mohan, Shri M. Karthikeyan, Shri K. Ramesh, Shri Shaik Rafee, Shri L. Mohanasundaram, Shri L. Muthu, Shri N. Sreenivas, Shri L. Eagambaram, Shri D. Muralidhar, Shri S. Ravishankar, Shri S. Alexander Xavier, Shri C. Rajappan, Shri K. Ganesh, Shri Ashish Tiwari, Shri P. R. Ashokkumar, Shri K. Arumugam, Shri Shiv Prakash Ruhela, Shri R. K. Mourya, Shri R. Ramalingam, Shri Vijay Tirkey, Shri P. Sonai, Shri M. Kathiravan, Shri K. A. Bijoy, Shri A. Selvakumaran, Shri D. Laxman, Shri M. Anbuchelian, Shri N. Chakraborty, Ms. Indra G. Ramadoss from FRTG

Design, Numerical and Experimental Simulations, Development and Qualification of Principal Fuel Handling Machines of PFBR

Shri S. Raghupathy, RDG, IGCAR & Shri R. J. Patel, RD&DG, BARC - Group Leaders

Shri Jose Varghese, Shri A. Venkatesan, Shri N. Subramanian, Shri E. Balasundaram, Shri M. A. Sanjith, Ms. T. Suguna, Shri P. Shanmuganathi, Shri R. Suresh Kumar, Shri C. Ragavendran, Shri S. D. Sajish, Shri S. K. Rajesh, Shri M. Babu Rao, Shri R. Manu, Shri S. Ramesh, Shri M. Aravind, Shri G. Venkataiah, Shri V. Devaraj, Shri P. Raja, Shri V. Balasubramanian, Shri Sriramachandra Aithal, Shri Abhishek Mitra, Shri S. Saravanan, Ms. M. M. Shanthi, Shri P. Selvaraj, Dr. R. Gajapathy, Dr. K. Velusamy, Shri R. Arulbaskar, Shri K. Natesan, Shri S. Jalaldeen, Shri Bhuwan Chadra Sati, Shri Sanjay Kumar Pandey, Shri C. S. Surendran, Shri V. N. Sakthivel Rajan, Shri S. Arumugam, Shri Sanjeev Kumar, Shri P. Lennin, Shri L. Chadrasekaran, Shri S. Duraikannu from RDG, Shri S. Jaisankar, Shri G. Kempulraj, Shri B. S. Ramesh Babu, Shri M. Krishnamoorhy, Shri V. Praveen Kumar, Shri S. Parivallal, Shri S. A. Natarajan, Shri S. Murugan, Shri S. Satees Kumar, Shri C. Palani, Shri T. Saravanan, Shri D. Dileep, Shri U. Gunasekaran, Shri S. Ramesh, Shri G. Janarthanan, Shri V. Kodiarasan, Shri S. P. Jaisankar, Shri A. Padmanabhan, Shri S. Yuvaraj, Shri E. Venkatesan, Shri B. Ramalingam, Shri A. Gunasekaran, Shri P. Shanmugam from ESG, Shri B. K. Sreedhar, Shri G. Padmakumar, Shri S. C. S. P. Kumar Krovvidi, Shri Nilayendra Chakraborty, Shri Y. V. Nagaraja Bhat, Shri R. Nirmal Kumar, Shri S. Ignatius Sundar Raj, Shri P. Madan Kumar, Shri J. Saravanan, Shri R. Krishnamurthy, Shri M. Sambamurthy, Shri A. Kolanjiappan, Shri R. Ramalingam, Shri A. Sudarsana Rao, Shri P. Varadan, Shri Rakesh Kumar Mourya, Shri P. A. Kalaimannan, Shri N. Thulasi, Shri Anant Kumar, Shri T. V. Maran, Shri K. Mohanraj, Shri A. T. Loganathan, Shri D. Kuppusamy, Shri A. Anthuvan Clement, Shri S. Sureshkumar, Shri J. Jaikanth, Shri R. Shanmugam, Shri M. T. Janakiraman, Shri C. Adikesaven, Shri A. Ashok Kumar, Shri L. Muthu, Shri S. Bavanirajan, Shri B. K. Nashine, Shri P. R. Ashok Kumar, Shri L. Egambaram, Shri N. Sreenivas, Shri K. Arumgam, Shri A. Alexander Xavir, Shri P. Chenthil Velmurugan, Ms. M. Chandra, Shri G. Vijaya Kumar, Shri S. Chadramouli, Shri R. Rajendra Prasad, Shri D. Muralidhar, Shri S. Ravishankar, Shri J. Prabhakaran, Shri R. Parandaman, Shri N. Mohan, Shri R. Iyappan, Shri K. Ramesh, Shri Sheik Rafee, Shri M. Karthikeyan, Shri V. Kumaraswamy, Shri Gautam Anand, Shri D. K. Saxena, Shri B. Veeraraghavan, Shri C. Rajappan, Shri S. Kannan, Shri R. Punniyamurthy, Shri S. Krishnakumar, Shri R. Arjunan, Shri K. Ganesh, Shri Vijay Sharma, Shri Ashish Tiwari, Shri L. Mohanasundaram, Shri Parmanand Kumar, Shri N. Venkatesan, Shri Pabbineedi Lakshmayya, Shri P. Pothi, Shri A. Thirunavukarau, Shri V. Ramakrishnan, Shri K. Jayagopi, Shri D. Laxman, Shri P. Sonai, Shri S. Shanmugam, Shri R. Rajendran, Shri H. Rafiq Basha, Shri J. Prem, Shri M. Kathiravan, Shri V. Gunasekaran, Shri N. S. Shivakumar, Shri Gautam Kumar Pandey, Shri P. Lijukrishnan, Shri Vijay Singh Sikarwar, Shri S. Sathishkumar, Shri Nagaraju Bekkenti, Shri K.H. Anub, Shri N. Mariappan, Shri Asif Ahmad Bhat, Shri V. Nandakumar, Shri R. Nagaraj, Shri K. Thanigairaj, Shri L. S. Sivakumar, Shri S. P. Pathak, Shri P. Narayana Rao, Shri Sukanta Kumar Roy, Shri B. Babu, Ms. M. Mohana, Shri M. V. Subramanya Deepak, Shri Chandra Sekhar Singh, Shri T. Chandran, Shri J. Vincent, Dr. J. L. Sylvia, Shri P. Vijaya Mohana Rao, Shri V. S. Krishnaraj, Shri M. Anbuchelian, Ms. S. Divya, Ms. S. Nagajothi, Shri G. Anandan, Shri P. Bakthavatchalam, Shri C. Ambujakshanan Nair, Shri A. Kulanthai, Shri R. Gunasekaran, Shri V. Krishnamoorthy, Shri Pitambar Padhan, Ms. Indira G. Ramadoss from FRTG, Dr. Arun Kumar Bhaduri, Dr. Shaju K. Albert, Dr. Chittaranjan Das, Shri Hemant Kumar, Shri P. Chandrasekaran, Dr. S. D. Venugopal from MMG, Shri P. Rajasekar, Shri M. P. Prabhakar, Shri G. Vijayaraghavan, Ms. Alka Kumari from EIRSG, Shri N. Murugesan from CG, Shri N. Mahendran from FRFCF

The award was also shared by colleagues from BARC, BRIT and VECC

## Awards and Honours

Kalpakkam Community Radio Station (KCRS) was awarded second place under the category of best community radio program conducted by Anna University along with UNICEF

Dr. A. Ravishankar Project Director, FRFCF has been conferred with the INS Outstanding Service Award on Nuclear Fuel Cycle Technologies, including radiation safety and Environmental Protection

Dr. B. P. C. Rao has been conferred with International Recognition Award, by the Indian Society for NDT

Dr. Anish Kumar has been conferred with ISNT National NDT Award for Research and Development

Dr. S. Thirunavukkarasu has been conferred with ISNT National NDT Award for NDT Systems Innovation and Development

## Best Paper/Poster Award

Deployment of Wireless Sensor Network for Radiation Monitoring

Ms. Jemimah Ebenezer, Dr. S. A. V. Satya Murty

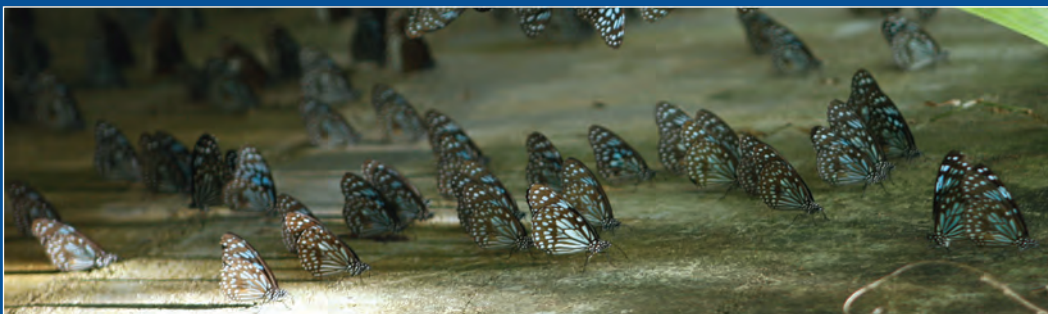
International Conference on Computing and Network Communications (CoCoNet'15) at IIITM-K, Trivandrum  
Best Paper Award

Theoretical Analysis on Designing Full Functional Device of WSN using Wireless Power Transfer

Ms. Vinita Daiya, Shri T. S. Shri Krishnan, Ms. G. Sandhya Rani, Ms. Jemimah Ebenezer, Dr. S. A. V. Satya Murty, Dr. B. P. C. Rao

12<sup>th</sup> IEEE India International Conference (INDICON 2015) at Jamia Millia Islamia, New Delhi

Best Paper Award



*Blue Tiger - Tirumala septentrionis*

**Dr. M. Sai Baba,**

Chairman, Editorial Committee, IGC Newsletter

Editorial Committee Members: Shri M. S. Chandrasekar, Dr. N. V. Chandra Shekar, Dr. T. S. Lakshmi Narasimhan  
Dr. C. Mallika, Shri V. Rajendran, Dr. Saroja Saibaba, Dr. C. V. Srinivas and Dr. Vidya Sundararajan